

RESEARCH ARTICLE

In vivo recombination of *Saccharomyces eubayanus* maltose-transporter genes yields a chimeric transporter that enables maltotriose fermentation

Nick Brouwers¹✉‡, Arthur R. Gorter de Vries¹✉‡, Marcel van den Broek¹, Susan M. Weening¹, Tom D. Elink Schuurman¹✉‡, Niels G. A. Kuijpers², Jack T. Pronk¹, Jean-Marc G. Daran¹*

1 Department of Biotechnology, Delft University of Technology, Van der Maasweg 9, 2629HZ Delft, The Netherlands, **2** HEINEKEN Supply Chain B.V., Global Innovation and Research, Zoeterwoude, Netherlands

✉ These authors contributed equally to this work.

‡ These authors share first authorship on this work.

* j.g.daran@tudelft.nl



OPEN ACCESS

Citation: Brouwers N, Gorter de Vries AR, van den Broek M, Weening SM, Elink Schuurman TD, Kuijpers NGA, et al. (2019) *In vivo* recombination of *Saccharomyces eubayanus* maltose-transporter genes yields a chimeric transporter that enables maltotriose fermentation. PLoS Genet 15(4): e1007853. <https://doi.org/10.1371/journal.pgen.1007853>

Editor: Jianzhi Zhang, University of Michigan, UNITED STATES

Received: September 27, 2018

Accepted: November 26, 2018

Published: April 4, 2019

Copyright: © 2019 Brouwers et al. This is an open access article distributed under the terms of the [Creative Commons Attribution License](https://creativecommons.org/licenses/by/4.0/), which permits unrestricted use, distribution, and reproduction in any medium, provided the original author and source are credited.

Data Availability Statement: All genome sequencing data files are available from the NCBI database (accession number Bioproject: PRJNA492251). Underlying numerical data for all graphs and summary statistics are provided in Supplementary data files 1 to 10.

Funding: This work was performed within the BE-Basic R&D Program (<http://www.be-basic.org/>), which was granted a TKI subsidy from the Dutch

Abstract

Saccharomyces eubayanus is the non-*S. cerevisiae* parent of the lager-brewing hybrid *S. pastorianus*. In contrast to most *S. cerevisiae* and Froberg-type *S. pastorianus* strains, *S. eubayanus* cannot utilize the α -tri-glucoside maltotriose, a major carbohydrate in brewer's wort. In *Saccharomyces* yeasts, utilization of maltotriose is encoded by the subtelomeric *MAL* gene family, and requires transporters for maltotriose uptake. While *S. eubayanus* strain CBS 12357^T harbors four *SeMALT* genes which enable uptake of the α -di-glucoside maltose, it lacks maltotriose transporter genes. In *S. cerevisiae*, sequence identity indicates that maltotriose and maltose transporters likely evolved from a shared ancestral gene. To study the evolvability of maltotriose utilization in *S. eubayanus* CBS 12357^T, maltotriose-assimilating mutants obtained after UV mutagenesis were subjected to laboratory evolution in carbon-limited chemostat cultures on maltotriose-enriched wort. An evolved strain showed improved maltose and maltotriose fermentation in 7 L fermenter experiments on industrial wort. Whole-genome sequencing revealed a novel mosaic *SeMALT413* gene, resulting from repeated gene introgressions by non-reciprocal translocation of at least three *SeMALT* genes. The predicted tertiary structure of *SeMalT413* was comparable to the original *SeMalT* transporters, but overexpression of *SeMALT413* sufficed to enable growth on maltotriose, indicating gene neofunctionalization had occurred. The mosaic structure of *SeMALT413* resembles the structure of *S. pastorianus* maltotriose-transporter gene *SpMTY1*, which has high sequences identity to alternately *S. cerevisiae* *MALx1*, *S. paradoxus* *MALx1* and *S. eubayanus* *SeMALT3*. Evolution of the maltotriose transporter landscape in hybrid *S. pastorianus* lager-brewing strains is therefore likely to have involved mechanisms similar to those observed in the present study.

Ministry of Economic Affairs, Agriculture and Innovation (EL&I). The funders had no role in study design, data collection and analysis, decision to publish, or preparation of the manuscript.

Competing interests: I have read the journal's policy and the authors of this manuscript have the following competing interests: TDES and NGAK are employees of the beer brewing company HEINEKEN B.V. NB, ARGdV, NGAK and JMGD are inventors of a patent application related to this work. The remaining authors declare no competing interests.

Author summary

Fermentation of the wort sugar maltotriose is critical for the flavor profile obtained during beer brewing. The recently discovered yeast *Saccharomyces eubayanus* is gaining popularity as an alternative to *S. pastorianus* and *S. cerevisiae* for brewing, however it is unable to utilize maltotriose. Here, a combination of non-GMO mutagenesis and laboratory evolution of the *S. eubayanus* type strain CBS 12357^T was used to enable maltotriose fermentation and improve brewing performance. The improved strain expressed a novel transporter gene, *SeMALT413*, which was formed by recombination between three different *SeMALT* maltose-transporter genes. Overexpression of *SeMALT413* in CBS 12357^T confirmed its neofunctionalization as a maltotriose transporter. As the *S. pastorianus* maltotriose transporter *SpMty1* has a mosaic structure similar to *SeMALT413*, maltotriose utilization likely involved similar recombination events during the domestication of current lager brewing strains. Based on a posteriori sequence analysis, the emergence of gene functions has been attributed to gene neofunctionalization in a broad range of organisms. The real-time observation of neofunctionalization during laboratory evolution constitutes an important validation of the relevance and importance of this mechanism for Darwinian evolution.

Introduction

Saccharomyces eubayanus was discovered in Patagonia and identified as the non-*S. cerevisiae* parental species of hybrid *S. pastorianus* lager-type beer brewing yeasts [1,2]. While *S. cerevisiae* is strongly associated with biotechnological processes, including dough leavening, beer brewing and wine fermentation [3], *S. eubayanus* has only been isolated from the wild [4–6]. Beer brewing is performed with wort, a complex substrate containing a fermentable sugar mixture of 15% of the monosaccharide glucose, 60% of the α -di-glucoside maltose and 25% of the α -tri-glucoside maltotriose [7]. While many *S. cerevisiae* and *S. pastorianus* strains utilize all three sugars, *S. eubayanus* isolates do not utilize maltotriose [8–10]. In *Saccharomyces*, the ability to utilize maltotriose requires its uptake into the cell and subsequent hydrolysis into glucose [11,12]. Maltose and maltotriose utilization are encoded by genes clustered in the *MAL* loci, which can be present on up to five different chromosomes [13]. *MAL* loci typically harbor genes from up to three gene families (Fig 1): a *MALT* polysaccharide proton-symporter gene, a *MALS* α -glucosidase gene which hydrolyses α -oligo-glucosides into glucose, and a *MALR* regulator gene that induces the transcription of *MALT* and *MALS* genes in the presence of maltose [14]. While *MALS* genes enable hydrolysis of both maltose and maltotriose, the *MALT* gene family comprises transporters with diverse substrate specificities [11,15]. In *S. cerevisiae*, most *MAL* loci harbor an *ScMalx1* transporter (Fig 1), which transports maltose and other disaccharides, such as turanose and sucrose [12,16], but cannot import maltotriose [11]. In contrast, the *MAL1* locus located on chromosome VII of *S. cerevisiae* contains *ScAGT1*, a transporter gene with only 57% nucleotide identity with *ScMALx1* transporter genes. *ScAGT1* encodes a broad-substrate-specificity sugar-proton symporter that enables maltotriose uptake [11,17,18].

The *S. eubayanus* type strain CBS 12357^T is able to utilize maltose, but cannot utilize maltotriose, suggesting that it expresses a functional maltase and a functional maltose transporter, but no maltotriose transporter [9]. Indeed, the four *MAL* loci in CBS 12357^T harbor a total of two *MALS* genes and four *MALT* genes with high homology to *ScMALx1*: *SeMALT1*, *SeMALT2*, *SeMALT3* and *SeMALT4* (Fig 1) [20]. Deletion of these genes in *S. eubayanus* type

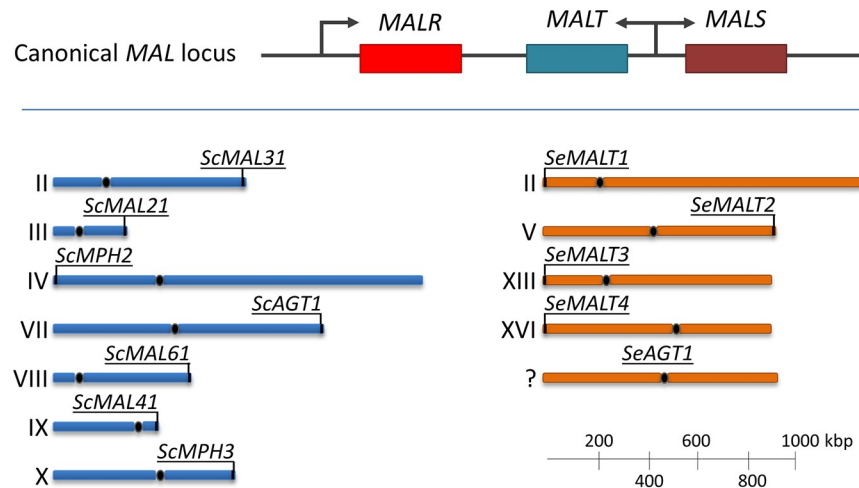


Fig 1. Organization of maltose and maltotriose transporter genes in *S. cerevisiae* and *S. eubayanus*. In *Saccharomyces* species, maltose and maltotriose utilization is encoded in the *MAL* genes, which are located in subtelomeric regions and comprise three types of genes: a *MALT* α -oligo-glucoside proton-symporter gene, a *MALS* α -glucosidase gene which hydrolyses α -(di or tri)-glucosides into glucose, and a *MALR* regulator gene that induces the transcription of *MALT* and *MALS* genes in the presence of maltose. In canonical *MAL* loci, the *MALT* and *MALS* are expressed from a bi-directional *MALR*-dependent promoter sequence. The chromosomal location of known maltose and maltotriose transporter genes in *S. cerevisiae* and *S. eubayanus* is shown, although the presence of these genes varies among isolates. *ScMPH2* and *ScMPH3* encode α -glucoside permeases which do not enable efficient maltotriose uptake [11]. *ScMAL31*, *ScMAL21*, *ScMAL61* and *ScMAL41* encode maltose transporters of the ScMalx1 family. *ScAGT1* encodes a maltotriose transporter. *SeMALT1*, *SeMALT2*, *SeMALT3* and *SeMALT4* encode maltose transporters with high sequence identity to the ScMalx1 family. *SeAGT1* is a maltotriose transporter which has recently been discovered in the north American *S. eubayanus* isolate yHRVM108 [19].

<https://doi.org/10.1371/journal.pgen.1007853.g001>

strain CBS 12357^T indicated that its growth on maltose relies on expression of *SeMALT2* and *SeMALT4* [9]. *SeMALT1* and *SeMALT3* were found to be poorly expressed in the presence of maltose in this strain, supposedly due to incompleteness of the *MAL* loci which harbor them. However, no homolog of *ScAGT1* was found in the genome of CBS 12357^T, and neither CBS 12357^T nor its derivatives overexpressing *SeMALT* genes were able to utilize maltotriose [9].

The *MALT* transporter genes in *Saccharomyces* yeasts are localized to the subtelomeric regions (Fig 1) [9,11,12,20–22], which are gene-poor and repeat-rich sequences adjacent to the telomeres [23–25]. The presence of repeated sequences makes subtelomeric regions genetically unstable by promoting recombination [26,27]. As a result, subtelomeric gene families are hot-spots of genetic diversity [28–30]. In *S. cerevisiae*, subtelomeric gene families contain more genes than non-subtelomeric gene families, reflecting a higher incidence of gene duplications [28]. As previously shown in *Candida albicans* submitted to long term laboratory evolution, the gene repertoire of the subtelomeric *TLO* family can be extensively altered due to ectopic recombinations between subtelomeric regions of different chromosomes, resulting in copy number expansion, in gene disappearance and in formation of new chimeric genes [31]. Despite their common origin, genes within one family can have different functions, due to the accumulation of mutations [32,33]. *In silico* analysis of the sequences and functions of genes from the *MALT*, *MALS* and *MALR* gene families indicated functional diversification through gene duplication and mutation [28]. Gene duplication is a critical step for the evolution of new gene functions [34,35]. Indeed, the presence of multiple gene copies can facilitate the emergence of advantageous mutations mainly by one of three mechanisms: (i) neofunctionalization, corresponding to the emergence of a novel function which was previously absent in the gene family [36], (ii) subfunctionalization, corresponding to the specialization of gene copies

for part of the function of the parental gene [37] and (iii) altered expression due to gene dosage effects resulting from the increased copy number [38]. While the different functions of *MALS* genes were assigned to subfunctionalization of the ancestral *MALS* gene [15], it is not known how the different functions of the maltotriose transporter gene *ScAGT1* and of other maltose transporter genes of the *MALT* family evolved from a common ancestor gene [28]. In general, the emergence of a large array of gene functions was attributed to subfunctionalization and neofunctionalization [15,28,31,39–42]. However, current evidence for neofunctionalization within subtelomeric gene families is based on *a posteriori* analysis and rationalization of existing sequence diversity. While in some cases the genetic process leading to neofunctionalization could be reconstructed at the molecular level [42–44], the emergence of a completely new function within a subtelomeric gene family was never observed within the timespan of an experiment to the best of our knowledge. However, the genetic diversity within *Saccharomyces MALT* transporters suggests that evolution of *SeMalT* transporters could lead to the emergence of a maltotriose transporter by neofunctionalization [28]. Therefore, laboratory evolution may be sufficient to obtain maltotriose utilization in *S. eubayanus* strain CBS 12357^T.

Laboratory evolution is a commonly-used method for obtaining desired properties by prolonged growth and selection under conditions favoring cells which develop the desired phenotype [45,46]. Similarly as in Darwinian natural evolution, the conditions under which laboratory evolution is conducted shape the phenotypes acquired by evolved progeny following the process of survival of the fittest [47]. In *Saccharomyces* yeasts, selectable properties include complex and diverse phenotypes such as high temperature tolerance, efficient nutrient utilization and inhibitor tolerance [48–51]. Laboratory evolution was successfully applied to improve sugar utilization for arabinose, galactose, glucose and xylose [49,52–54]. In *S. pastorianus*, improved maltotriose uptake was successfully selected for in a prolonged chemostat cultivation on medium enriched with maltotriose [55]. Theoretically, laboratory evolution under similar conditions could select *S. eubayanus* mutants which develop the ability to utilize maltotriose.

In this study, we submitted *S. eubayanus* strain CBS 12357^T to UV-mutagenesis and laboratory evolution in order to obtain maltotriose utilization under beer brewing conditions. While obtaining a non-GMO maltotriose-consuming *S. eubayanus* strain was a goal in itself for industrial beer brewing, we were particularly interested in the possible genetic mechanisms leading to the emergence of maltotriose utilization. Indeed, we hypothesized that the genetic plasticity and functional redundancy of the four subtelomeric *SeMALT* genes of CBS 12357^T could facilitate the emergence of maltotriose transport by neofunctionalization. The evolution process leading to maltotriose utilization in a strain with only maltose transporters, such as CBS 12357^T, may provide insight in the emergence of maltotriose utilization in general.

Results

Mutagenesis and evolution enables *S. eubayanus* to utilize maltotriose

To obtain maltotriose-consuming mutants, CBS 12357^T was grown on synthetic medium containing 20 g L⁻¹ glucose (SMG) until stationary phase, and approximately 10⁸ cells were used to inoculate synthetic medium containing 20 g L⁻¹ maltotriose (SMMt) as sole carbon source. After incubation at 20°C for three months, neither growth nor maltotriose utilization was observed.

Exposure to UV-radiation can cause DNA damage, resulting in the emergence of cells with diverse mutations due to error-prone repair. Therefore, UV-mutagenesis was applied to increase the likelihood of obtaining a mutation enabling maltotriose utilization. To this end, CBS 12357^T was grown in SMG medium, sporulated, submitted to mild UV-mutagenesis

(46% survival rate) and approximately 10^8 cells of the mutagenized population were used to inoculate SMMt containing 20 g L^{-1} maltotriose. After two weeks at 20°C , growth was observed and, after 3 weeks, the maltotriose concentration had decreased to 10.5 g L^{-1} . After two subsequent transfers in fresh SMMt, 96 single cells were sorted into a 96 well plate containing YPD medium by fluorescence-activated cell sorting (FACS). The resulting single-cell cultures were transferred to a 96 well plate containing SMMt, in which growth was monitored by OD_{660} measurements. The seven single-cell isolates with the highest final OD_{660} were selected and named IMS0637-IMS0643. To characterize growth on maltotriose, the strain CBS 12357^T, the single-cell isolates IMS0637-IMS0643 and the maltotriose-consuming *S. pastorianus* strain CBS 1483 were grown in shake flasks on SMMt (Fig 2A and S1 Fig). After 187 h, *S. eubayanus* CBS 12357^T did not show any maltotriose consumption. Conversely, isolates IMS0637-IMS0643, all showed over 50% maltotriose consumption after 91 h (as compared to 43 h for CBS 1483). Upon reaching stationary phase, isolates IMS0637-IMS0643 had consumed $93 \pm 2\%$ of the initial maltotriose concentration, which was similar to the 92%

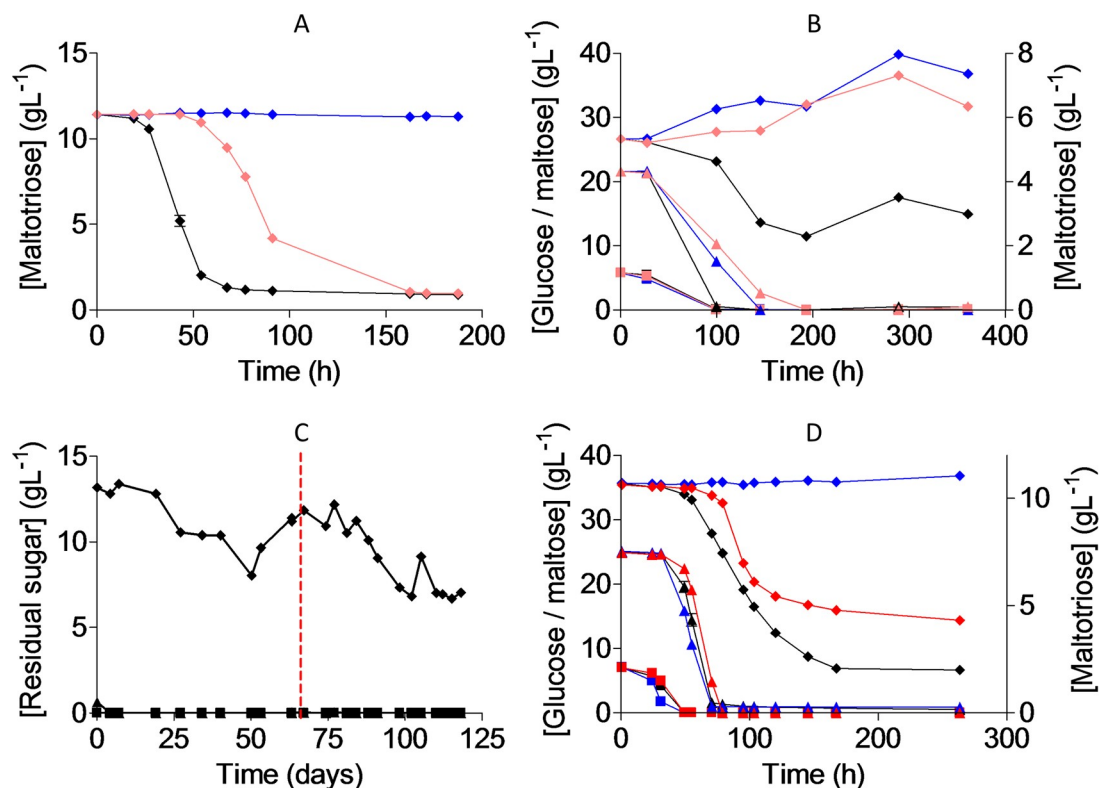


Fig 2. Mutagenesis and evolution to obtain maltotriose consuming *S. eubayanus*. (A) Characterization of *S. pastorianus* CBS 1483 (black), *S. eubayanus* CBS 12357^T (blue) and IMS0637 (light red) on SMMt at 20°C . The data for IMS0637 is representative for the other mutants IMS0638-IMS0643 (S1 Fig). The average concentration of maltotriose (diamonds) and average deviation were determined from two replicates (S2 Data File). (B) Characterization of *S. pastorianus* CBS 1483 (black), *S. eubayanus* CBS 12357^T (blue) and IMS0637 (light red) on wort at 20°C . The concentrations of glucose (squares), maltose (triangles) and maltotriose (diamonds) were measured from single biological measurements (S3 Data File). (C) Residual maltotriose concentration in the outflow during laboratory evolution of strains IMS0637-IMS0643 in an anaerobic chemostat at 20°C on maltotriose enriched wort. The concentrations of glucose (squares), maltose (triangles) and maltotriose (diamonds) were measured by HPLC. The chemostat was restarted after a technical failure (red dotted line, S4 Data File). (D) Characterization of *S. pastorianus* CBS 1483 (black), *S. eubayanus* CBS 12357^T (blue) and IMS0750 (red) on wort at 12°C in 250 mL micro-aerobic Neubar infusion bottles. The average concentration and standard deviation of glucose (squares), maltose (triangles) and maltotriose (diamonds) were determined from three biological replicates. The data for IMS0751 and IMS0752 are shown in S5 Data File and S2 Fig.

<https://doi.org/10.1371/journal.pgen.1007853.g002>

conversion reached by *S. pastorianus* CBS 1483. While these results indicated that the single cell isolates IMS0637-IMS0643 utilized maltotriose in synthetic medium, they did not consume maltotriose in presence of glucose and maltose after 145 h of incubation (Fig 2B). Under the same conditions, *S. pastorianus* CBS 1483 consumed 50% of the maltotriose after 145 h (Fig 2B).

Nutrient-limited growth confers a selective advantage to spontaneous mutants with a higher nutrient affinity [45,55]. Therefore, to improve maltotriose utilization under industrially-relevant conditions, the pooled isolates IMS0637-IMS0643 were subjected to laboratory evolution in a chemostat culture on modified brewer's wort. To avoid the presence of residual maltose, which would prevent selection for maltotriose utilization, brewer's wort was diluted 6-fold. To strengthen the selective advantage for maltotriose-consuming cells, the diluted wort was complemented with 10 g L⁻¹ maltotriose, yielding concentrations of 2 g L⁻¹ glucose, 15 g L⁻¹ maltose and 15 g L⁻¹ maltotriose in the medium feed. To prevent growth limitation due to the availability of limited oxygen or nitrogen, the medium was supplemented with 10 mg L⁻¹ ergosterol, 420 mg L⁻¹ Tween 80 and 5 g L⁻¹ ammonium sulfate [56]. During the batch cultivation phase that preceded continuous chemostat cultivation, glucose and maltose were completely consumed, leaving maltotriose as the only carbon source. After initiation of continuous cultivation at a dilution rate of 0.03 h⁻¹, the medium outflow initially contained 13.2 g L⁻¹ of maltotriose. After 121 days of chemostat cultivation, the maltotriose concentration had progressively decreased to 7.0 g L⁻¹ (Fig 2C). At that point, which corresponded to *ca.* 125 generations, 10 single colonies were isolated from the culture on SMMt agar plates and incubated at 20°C. Three single-cell lines were named IMS0750, IMS0751 and IMS0752 and selected for further characterization in micro-aerobic cultures, grown at 12°C on 3-fold diluted wort, along with *S. eubayanus* CBS 12357^T and *S. pastorianus* CBS 1483 (Fig 2D). In these cultures, strains CBS 12357^T and IMS0751 only consumed glucose and maltose, while *S. pastorianus* CBS 1483, as well as the evolved isolates IMS0750 and IMS0752, also consumed maltotriose (S2 Fig). After 263 h, maltotriose concentrations in cultures of strains IMS0750 and IMS0752 had decreased from 10.7 to 4.3 g L⁻¹ maltotriose as compared to 2.0 g L⁻¹ in cultures of strain CBS 1483.

Whole genome sequencing reveals a new recombined chimeric *SeMALT* gene

We sequenced the genomes of the *S. eubayanus* strain CBS 12357^T, of the UV-mutagenized isolates IMS0637-IMS0643 and of the strains isolated after subsequent chemostat evolution IMS0750-IMS0752 using paired-end Illumina sequencing. Sequencing data were mapped to a chromosome-level assembly of strain CBS 12357^T [9] to identify SNPs, INDELS and copy number changes. The genomes of the UV-mutants IMS0637, IMS0640, IMS0641 and IMS0642 shared a set of 116 SNPs, 5 INDELS and 1 copy number variation (S1 Data File). In addition to these shared mutations, isolates IMS0638, IMS0639 and IMS0643 carried three identical SNPs. Overall, 97% of SNPs and INDELS of IMS0637-IMS0643 were heterozygous, indicating that the haploid spores of CBS 12357^T diploidized by mating after mutagenesis (S1 Data File). Of the mutations present in all isolates, 34 SNPs and all 5 INDELS affected intergenic regions, 30 SNPs were synonymous, 48 SNPs resulted in amino acid substitutions and 4 SNPs resulted in a premature stop codon (S1 Data File). None of the 52 non-synonymous SNPs affected genes previously linked to maltotriose utilization. The only copy number variation concerned a duplication of the right subtelomeric region of CHRVIII. Read mate-pairing indicated that the duplicated region was attached to the left arm of CHRII, causing the

replacement of left subtelomeric region of CHRII by a non-reciprocal translocation. The recombination resulted in loss of one of the *SeMALT1* allele, which is not expressed in CBS 12357^T [9].

Since the ability to utilize maltotriose in wort emerged only after laboratory evolution during chemostat cultivation, mutations present in the chemostat-evolved strains IMS0750 and IMS0752 were studied in more detail. With the exception of one synonymous SNP, IMS0750 and IMS0752 were identical and shared 100 SNPs, 3 INDELS and 5 copy number changes (S1 Data File). The non-maltotriose utilizing strain IMS0751 shared only 63 SNPs and 3 INDELS with IMS0750 and IMS0752, of which 98% were homozygous, indicating a recent loss of heterozygosity event affected its entire genome. Of the mutations in maltotriose-utilizing strains IMS0750 and IMS0752, only 5 SNPs and 4 copy number changes were absent in IMS0637-IMS0643, and could therefore explain the ability to utilize maltotriose in wort (Fig 3A). The 5 SNPs consisted of two intergenic SNPs and three non-synonymous SNPs in genes with no link to maltotriose. However, the changes in copy number affected several regions harboring *SeMALT* genes: a duplication of 550 bp of CHRII including *SeMALT1* (coordinates 8,950 to 9,500), a duplication of the left arm of CHR XIII including *SeMALT3* (coordinates 1–10,275), loss of the left arm of CHR XVI (coordinates 1–15,350), and loss of 5.5 kb of CHR XVI including *SeMALT4* (coordinates 16,850–22,300). Analysis of read mate pairing indicated that the copy number variation resulted from a complex set of recombinations between chromosomes II, XIII and XVI.

The high degree of sequence identity of the affected *MAL* loci and their localization in the subtelomeric regions made exact reconstruction of the mutations difficult. Therefore, IMS0637 and IMS0750 were sequenced using long-read sequencing on ONT's MinION platform, and a *de novo* genome assembly was made for each strain. Comparison of the resulting assemblies to the chromosome-level assembly of CBS 12357^T indicated that two recombinations had occurred. Both in IMS0637 and IMS0750, an additional copy of the terminal 11.5 kb of the right arm of chromosome VIII had replaced the terminal 11.4 kb of one of the two copies of the left arm of chromosome II (Fig 3B). This recombination was consistent with the copy number changes of the affected regions in IMS0637-IMS0643, IMS0750 and IMS0752 and resulted in the loss of one copy of the *MAL* locus harboring *SeMALT1*. In addition, the genome assembly of IMS0750 indicated the replacement of both copies of the first 22.3 kb of CHR XVI by complexly rearranged sequences from CHRII, CHR XVIII and CHR XVI. The recombined region comprised the terminal 10,273 nucleotides of the left arm of CHR III, followed by 693 nucleotides from CHRII, 1,468 nucleotides from CHR XVI and 237 nucleotides from CHR XIII (Fig 3B). The recombinations were non reciprocal, as the regions present on the recombined chromosome showed increased sequencing coverage while surrounding regions were unaltered. This recombination resulted in the loss of the canonical *MAL* locus harboring *SeMALT4* on chromosome XVI. However, the recombined sequence contained a chimeric open reading frame consisting of the 5' part of *SeMALT4* from CHR XVI, the middle of *SeMALT1* from CHRII and the 3' part of *SeMALT3* from CHR XIII (Fig 3C, S3 Fig). To verify this recombination, the ORF was PCR amplified using primers binding on the promoter of *SeMALT4* and the terminator of *SeMALT3*, yielding a fragment for strain IMS0750, but not for CBS 12357^T and IMS0637. Sanger sequencing of the fragment amplified from strain IMS0750 confirmed the chimeric organization of the ORF, which we named *SeMALT413*. The sequence of *SeMALT413* showed 100% identity to *SeMALT4* for nucleotides 1–434 and 1113–1145, 100% identity to *SeMALT1* for nucleotides 430–1122 and 100% identity to *SeMALT3* for nucleotides 1141–1842 (Fig 3C). Nucleotides 1123–1140, which showed only 72% identity with *SeMALT1* and 61% identity with *SeMALT3*, were found to represent an additional introgression (Fig 3B). While the first 434 nucleotides can be unequivocally attributed to *SeMALT4*

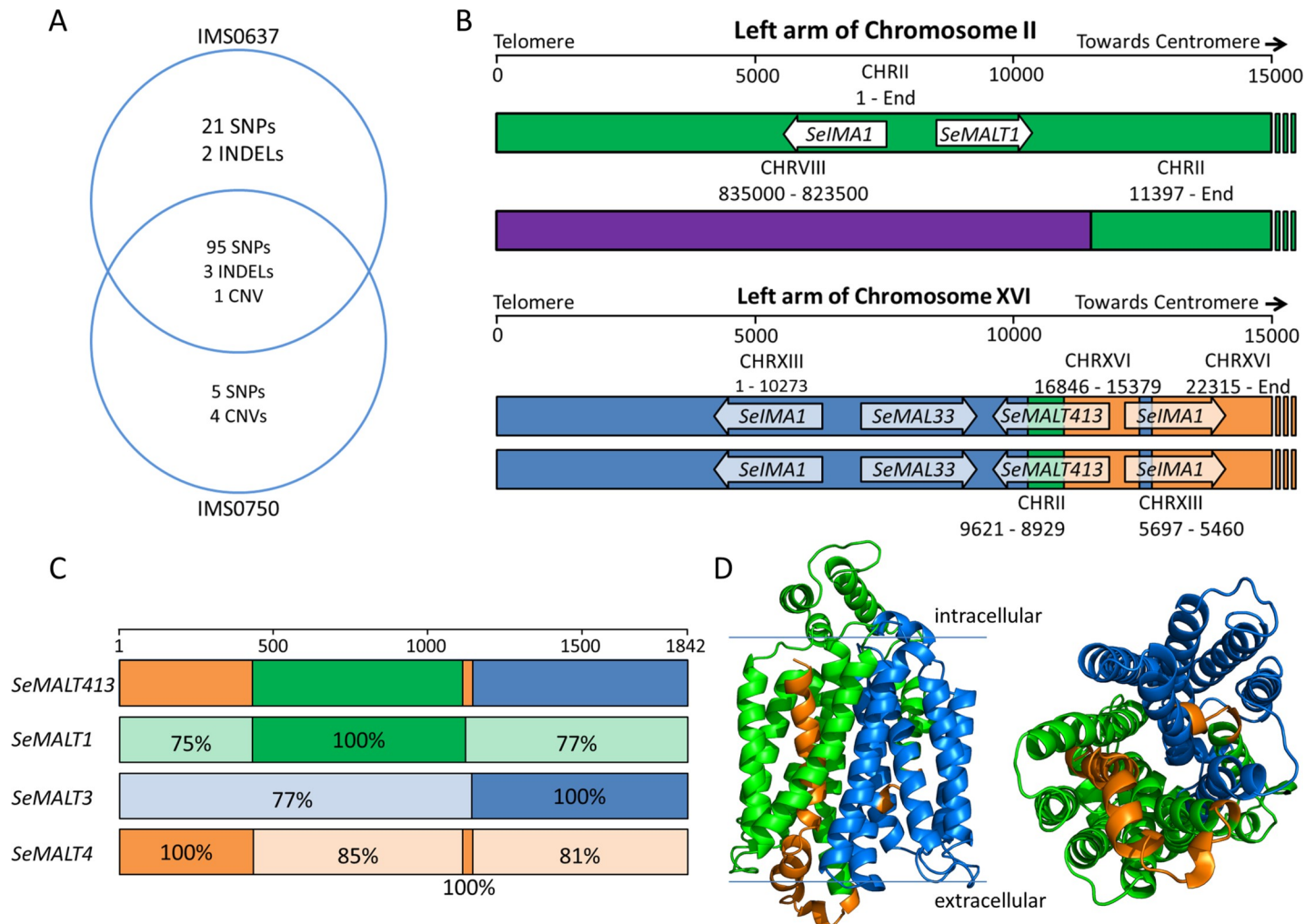


Fig 3. Identification of mutations in the mutagenized strain IMS0637 and the evolved strain IMS0750. (A) Venn diagram of the mutations found in UV-mutagenized IMS0637 and evolved IMS0750 relative to wildtype CBS 12357^T. Single nucleotide polymorphisms (SNPs), small insertions and deletions (INDELS) and copy number variation (CNV) are indicated as detected by Pilon. (B) Recombined chromosome structures in IMS0637 and IMS0750 as detected by whole genome sequencing using MinION nanopore technology and *de novo* genome assembly. The first 15,000 nucleotides of the left arm of CHR II and CHR XVI are represented schematically. The origin of the sequence is indicated in green for CHR II, purple for CHR VIII, blue for CHR XIII and orange for CHR XVI. The ORFs of *SeMALT* transporter genes, *SeIMA* isomaltase genes and the *MALR*-type regulator *SeMAL33* which were affected by the recombinations are indicated by arrows. While the recombination of CHR II and CHR VIII was present in IMS0637 and IMS0750, the recombination of both copies of CHR XVI was found only in IMS0750 but not in IMS0637. The recombination on CHR XVI created the chimeric *SeMALT413* transporter gene. (C) Overview of the sequence identity of the 1,842 nucleotides of *SeMALT413* relative to *SeMALT1*, *SeMALT3* and *SeMALT4*. The open reading frames of the genes were aligned (S3 Fig) and regions with 100% sequence identity were identified. For regions in which the sequence identity was lower than 100%, the actual sequence identity is indicated for each *SeMALT* gene. The origin of the sequence is indicated in green for CHR II, red for CHR VIII, blue for CHR XIII and orange for CHR XVI. (D) Prediction of the protein structure of *SeMalT413* with on the left side a transmembrane view and on the right a transport channel view. Domains originated from *S. eubayanus* *SeMalT* transporters are indicated by the colors orange (*SeMalT4* chromosome XVI), green (*SeMalT1* chromosome II) and blue (*SeMalT3* chromosome XIII).

<https://doi.org/10.1371/journal.pgen.1007853.g003>

due to a nucleotide difference with *SeMALT2*, the nucleotides 1123–1140 are identical in *SeMALT2* and *SeMALT4*. Therefore, this part of the sequence of *SeMALT413* might have come from *SeMALT2* on CHR V or from *SeMALT4* on CHR XVI. Overall, *SeMALT413* showed a sequence identity of only 85 to 87% with the original *SeMALT* genes, with the corresponding protein sequence exhibiting between 52 and 88% similarity. We therefore hypothesized that the recombined *SeMalT413* transporter might have an altered substrate specificity and thereby enable maltotriose utilization.

The tertiary protein structure of the chimeric *SeMALT413* gene was predicted with SWISS-MODEL (<https://swissmodel.expasy.org/>), based on structural homology with the *Escherichia coli* xylose-proton symporter Xyle [57], which has previously been used as a reference to model the structure of the maltotriose transporter *ScAgt1* [58]. Similarly to the maltose transporters in *Saccharomyces*, Xyle is a proton symporter belonging to the major facilitator superfamily with a transmembrane domain composed of 12 α -helices (S4 Fig). The same structure was predicted for *SeMalT413*, with 1 α -helix formed exclusively by residues from *SeMalT4*, 4 α -helices formed exclusively by residues from *SeMalT1* and 5 α -helices formed exclusively by residues from *SeMalT3* (Fig 3D). The remaining two α -helices were composed of residues from more than one transporter. Since the first 100 amino acids were excluded from the model due to absence of similar residues in the xylose symporter reference model, the structure prediction underestimated the contribution of *SeMalT4*. The three-dimensional arrangement of the α -helices of *SeMalT413* was almost identical to *SeMalT1*, *SeMalT3* and *SeMalT4*, indicating that it retained the general structure of a functional maltose transporter (S5 Fig).

Introduction of the *SeMALT413* gene in wildtype CBS 12357^T enables maltotriose utilization

The small structural differences identified between *SeMalT413* and the wild-type *S. eubayanus* *SeMalT* transporters could not be used to predict the ability of *SeMalT413* to transport maltotriose [58]. Therefore, to investigate its role in maltotriose transport, *SeMALT413* and, as a control, *SeMALT2* were overexpressed in the wild-type strain *S. eubayanus* CBS 12357^T (Fig 4A and S6 Fig). Consistently with previous gene editing in CBS 12357^T [9], the expression cassettes were inserted at the *SeSGA1* locus, encoding an intracellular sporulation-specific glucosylase which is not expressed during vegetative growth [59,60]. Growth of the resulting strains *S. eubayanus* IMX1941 (*SeSGA1* Δ ::*ScTEF1*_p-*SeMALT2*-*ScCYC1*_t) and IMX1942 (*SeSGA1* Δ ::*ScTEF1*_p-*SeMALT413*-*ScCYC1*_t), as well as the wild-type strain CBS 12357^T and the evolved isolate IMS0750 was tested on SM supplemented with different carbon sources (S7 Fig). On glucose, strains IMX1941 and IMX1942 exhibited the same specific growth rate of $0.25 \pm 0.01 \text{ h}^{-1}$ as CBS 12357^T, while IMS0750 grew faster with a growth rate of $0.28 \pm 0.01 \text{ h}^{-1}$. Glucose was completely consumed after 33 h (Fig 4B). On maltose, the specific growth rates of CBS 12357^T, IMX1941, IMX1942 and IMS0750 ranged between 0.17 and 0.19 h^{-1} and did not differ significantly. Maltose was completely consumed after 43 h (Fig 4C). On maltotriose, only the evolved mutant IMS0750 and reverse engineered strain IMX1942 (*ScTEF1*_p-*SeMALT413*-*ScCYC1*_t) showed growth. IMS0750 grew with a specific growth rate of $0.19 \pm 0.01 \text{ h}^{-1}$ and consumed 55% of maltotriose within 172 h. Over the same period, IMX1942 grew at $0.03 \pm 0.00 \text{ h}^{-1}$ and consumed 45% of the maltotriose after 172 h (Fig 4D), demonstrating the capacity of *SeMALT413* to transport maltotriose.

The *SpMTY1* maltotriose transporter gene displays a similar chimeric structure as *SeMALT413*

The emergence of the maltotriose transporter *SeMalT413* by recombination between different *MALT* genes during laboratory evolution demonstrates that *MALT* gene neofunctionalization can contribute to the emergence of maltotriose utilization. To investigate if such neofunctionalization could have played a role in the emergence of maltotriose transporter genes in *Saccharomyces* yeasts, we analyzed the sequences of existing maltotriose transporter genes in *S. cerevisiae* and *S. pastorianus* genomes. In *S. cerevisiae* strains, maltotriose transport is encoded by the *ScAGT1* gene [11,17,18]. However, *ScAGT1* is truncated and non-functional in *S. pastorianus* [61]. Instead, maltotriose utilization has been attributed to two *S. pastorianus*-specific

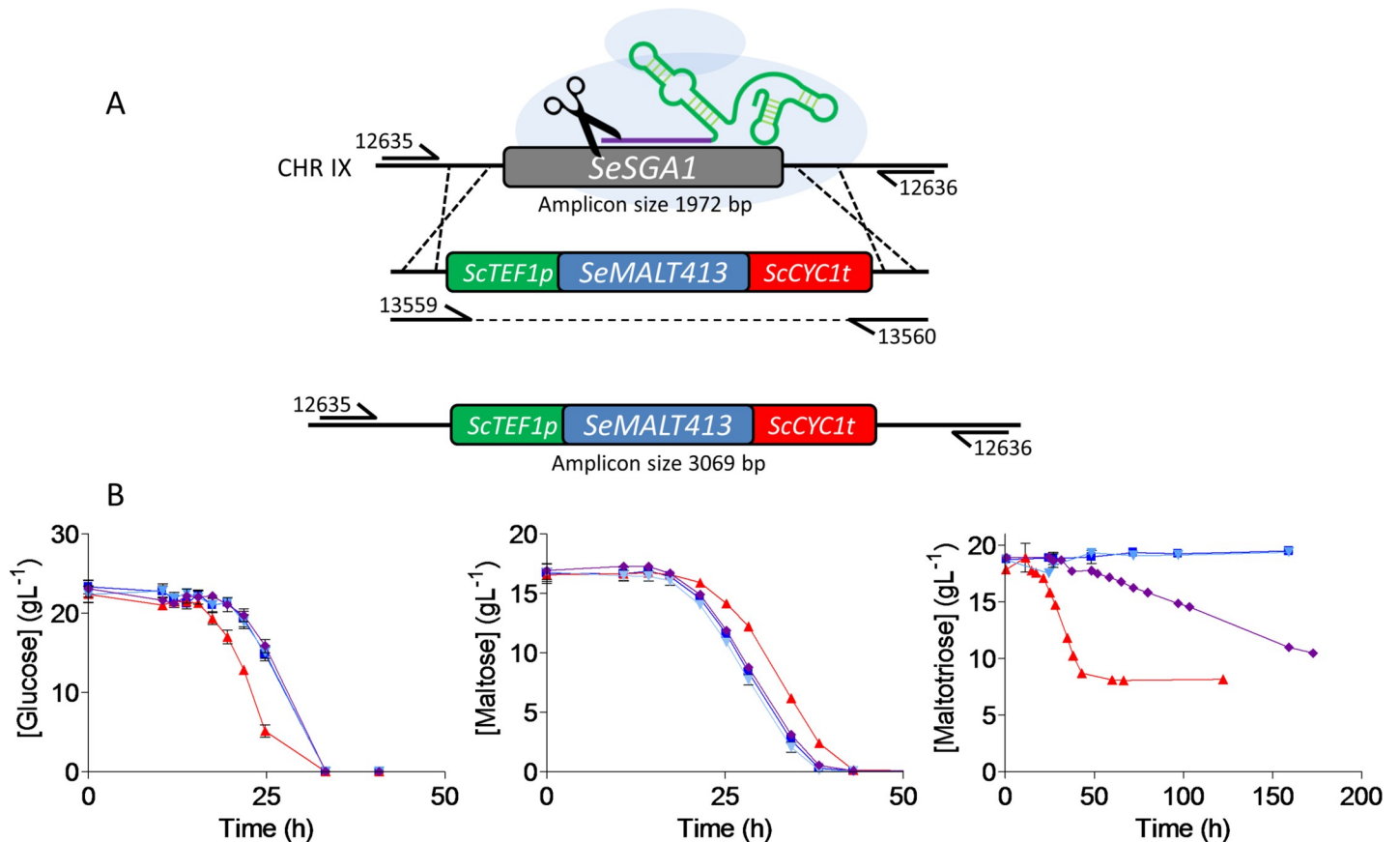


Fig 4. Reverse engineering of *SeMALT413* in CBS 12357^T and characterization of transporter functionality in SM. (A) Representation of the CRISPR-Cas9 gRNA complex (after self-cleavage of the 5' hammerhead ribozyme and a 3' hepatitis-δ virus ribozyme from the expressed gRNA) bound to the *SeSGA1* locus in CBS 12357^T. Repair fragment with transporter cassette *ScTEF1p-ScMALT413-ScCYC1t* was amplified from pUD814(*SeMALT413*) with primers 13559/13560 and contains overhangs with the *SeSGA1* locus for recombination. *SeSGA1* was replaced by the *ScTEF1p-ScMALT413-ScCYC1t* cassette. Correct transformants were checked using primers 12635/12636 upstream and downstream of the *SeSGA1* locus (S6 Fig). Strains were validated using Sanger sequencing. (B) Characterization of CBS 12357 (blue squares), IMS0750 (red triangles), IMX1941 (cyan triangles), IMX1942 (purple diamonds) on SM glucose, maltose and maltotriose. Strains were cultivated at 20°C and culture supernatant was measured by HPLC. Data represent average and standard deviation of three biological replicates (S6 Data File).

<https://doi.org/10.1371/journal.pgen.1007853.g004>

genes: *LgAGT1* and *SpMTY1*. The maltotriose transporter gene *LgAGT1* was identified on *S. eubayanus* chromosome XV of *S. pastorianus* and shares 85% sequence identity with *ScAGT1* [62,63]. Although it is absent in CBS 12357^T [20], *LgAGT1* was found to enable maltotriose transport in the north-American *S. eubayanus* isolate yHRVM108 [19,20]. The *SpMTY1* gene, also referred to as *MTT1*, was found in the *MAL1* locus of *S. pastorianus* [21,22]. In addition to *S. cerevisiae* chromosome VII, *SpMTY1* was also found on *S. eubayanus* chromosome VII of *S. pastorianus*, of which the right arm originates from *S. cerevisiae* due to a recombination [62]. *SpMTY1* shows 90% sequence identity with *ScMALx1* genes [21,22], but also displays segmental sequence identity with *SeMALT* genes [64,65].

The relatively low homology of *ScAGT1* and *LgAGT1* genes indicates that they are less related to maltose transporter genes such as *ScMALx1* and *SeMALT* than *SpMTY1*. Moreover, their sequence identity to maltose transporters from the *MALT* family such as *ScMAL31* is roughly homogenous over their coding region. Therefore there is no evidence that they resulted from recombinations between other *MALT* genes. In contrast, the identity of some segments of *SpMTY1* relative to *ScMAL31* deviates strongly from the average identity of 89% [21]. Indeed, sequence identity with *ScMAL31* of *S. cerevisiae* S288C [66] is above 98% for

nucleotides 1–439, 627–776, 796–845, 860–968 and 1,640–1,844, while it is only 79% for nucleotides 440–626, 65% for nucleotides 777–795, 50% for nucleotides 846–859 and 82% for nucleotides 969–1,639 (S8 Fig). Alignment of the sequences of *S. eubayanus* CBS 12357^T *SeMALT* genes [9] to *SpMTY1* showed high sequence identity with *SeMALT3* across several regions that showed significant divergence from the corresponding *ScMAL31* sequences: 91% identity for nucleotides 478–533, 94% identity for nucleotides 577–626 and 94% identity for nucleotides 778–794 (S8 Fig). These observations would indicate that the evolution of *SpMTY1* might have involved introgression events similar to those responsible for the *SeMALT413* neofunctionalization described in the present study. However, introgressions from *SeMALT* genes cannot explain the entire *SpMTY1* gene structure. Its evolution may therefore have involved multiple introgressions, similarly as for *SeMALT413*. While most regions with low identity to *ScMAL31* and *SeMALT3* were too short to identify their provenance, the sequence corresponding to the 969th to 1,639th nucleotide of *SpMTY1* could be blasted on NCBI. In the S288C genome, *ScMAL31* was the closest hit with 82% identity. However, when blasting the sequence against the full repository excluding *S. pastorianus* genomes, the closest hit was the orthologue of *ScMAL31* on chromosome VII of *S. paradoxus* strain YPS138. In addition to an 89% identity to nucleotides 969–1,639 of *SpMTY1*, *SparMAL31* had an identity of 94% for nucleotides 544–575 and of 93% for nucleotides 846–859 (S8 Fig). Therefore, the sequence of *SpMTY1* may have resulted from recombination between different *MALT* genes, involving *ScMALx1* and other *MALT* genes such as *SeMALT3* and *SparMAL31*. While the chimeric *SeMALT413* ORF can be fully explained by recombination between *SeMALT* genes, *SpMTY1* probably accumulated additional mutations during its evolution.

Applicability of a maltotriose-consuming *S. eubayanus* strain for lager beer brewing

S. eubayanus strains are currently used for industrial lager beer brewing [9]. To test the evolved strain IMS0750 under laboratory-scale brewing conditions, its performance was compared with that of its parental strain CBS 12357^T in 7 L cultures grown on high-gravity (16.6° Plato) wort (Fig 5). After 333 h, IMS0750 had completely consumed all glucose and maltose, and the concentration of maltotriose had dropped from 19.3 to 4.7 g L⁻¹ (Fig 5). In contrast, CBS 12357^T did not utilize any maltotriose. In addition to its improved maltotriose utilization, IMS0750 also showed improved maltose consumption: maltose was completely consumed within 200 h, while complete maltose consumption by strain CBS 12357^T took ca. 330 h (Fig 5). Consistent with its improved sugar utilization, the final ethanol concentration in cultures of strain IMS0750 was 18.5% higher than in corresponding cultures of strain CBS 12357^T (Fig 5). Brewing-related characteristics of IMS0750 were further explored by analyzing production of aroma-defining esters, higher alcohols and diacetyl. Final concentrations of esters and higher alcohols were not significantly different in cultures of the two strains, with the exception of isoamylacetate, which showed a 240% higher concentration in strain IMS0750 (Table 1). In addition, while the concentration of the off-flavour diacetyl remained above its taste threshold of 25 µg L⁻¹ after 333h for CBS 12357^T, it dropped below 10 µg L⁻¹ for IMS0750 (Table 1).

Discussion

UV-mutagenesis and subsequent laboratory evolution yielded mutants which were able to utilize maltotriose in synthetic medium and in brewer's wort. In the resulting isolates IMS0750 and IMS0752, several recombinations affecting subtelomeric regions were identified. All four maltose transporter genes in *S. eubayanus* CBS 12357^T are localized in subtelomeric *MAL* loci:

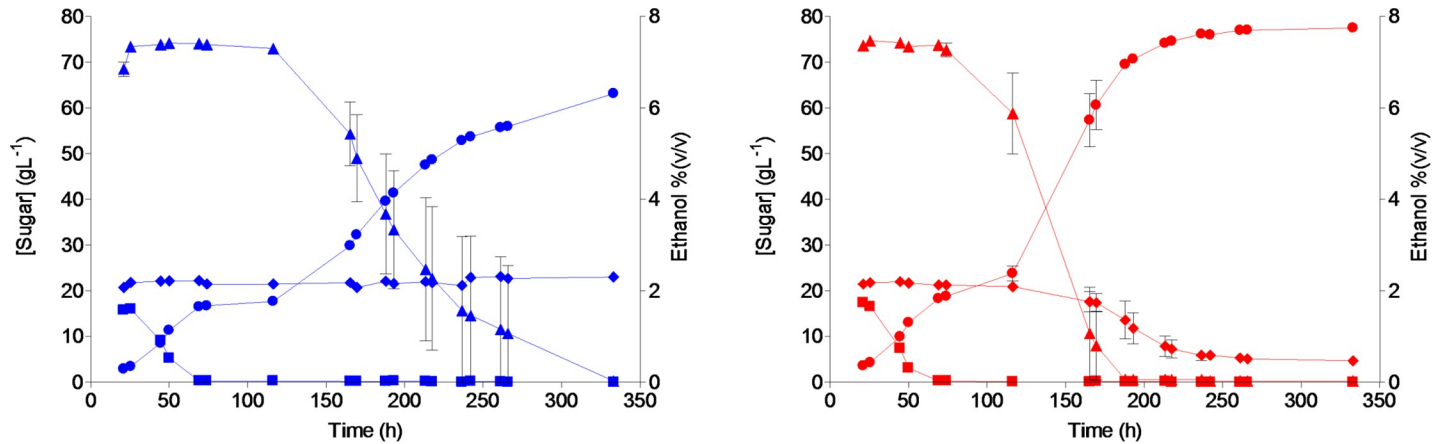


Fig 5. Extracellular metabolite profiles of *S. eubayanus* strains CBS 12357^T and IMS0750 in high-gravity wort at 7 L pilot scale. Fermentations were performed on wort with a gravity of 16.6° Plato. The average concentrations of glucose (squares), maltose (triangles), maltotriose (diamonds) and ethanol (circles) are shown for duplicate fermentations of CBS 12357^T (blue) and IMS0750 (red). The average deviations are indicated (S7 Data File).

<https://doi.org/10.1371/journal.pgen.1007853.g005>

SeMALT1 on chromosome II, *SeMALT2* on chromosome V, *SeMALT3* on chromosome XIII and *SeMALT4* on chromosome XVI [9,20]. In the evolved strain IMS0750, a complex recombination between the subtelomeric regions of chromosomes II, XIII and XVI involved at least three of these *MAL* loci. Long-read nanopore sequencing enabled complete reconstruction of the recombined left arm of chromosome XVI, revealing recombinations between the ORFs of at least *SeMALT1*, *SeMALT3* and *SeMALT4*. These recombinations occurred within the open reading frame of *SeMALT4* and the newly-formed chimeric ORF *SeMALT413* encoded a full length protein with a structure comparable to that of *SeMalT* transporters. In contrast to the original *SeMALT* genes, overexpression of *SeMALT413* enabled growth on maltotriose, indicating that *SeMalT413* acquired the ability to import maltotriose.

The predicted structure of *SeMalT413* was highly comparable to the structure of other transporters from the major facilitator superfamily [67] and to the structure of *SeMalT1*, *SeMalT3* and *SeMalT4*. While nothing is known about the amino acid residues responsible for substrate specificity in *SeMalT* transporters, the threonine and serine residues at the 505th and 557th position respectively of *ScAgt1* were identified as critical for maltotriose transport [68]. In *SeMalT413*, the corresponding amino acids originate from *SeMALT3*. However, since *SeMALT3* itself is unable to utilize maltotriose, the ability of *SeMalT413* to transport maltotriose likely depends on the interaction of residues from the different parental transporters, rather than from the residues of one of the transporters. Interestingly, CBS 12357^T was recently evolved for maltotriose utilization in another study, resulting in a chimeric *SeMALT434*

Table 1. Concentrations of alcohols, esters and diacetyl after fermentation of wort with a gravity of 16.6° P by *S. eubayanus* strains CBS 12357^T and IMS0750. The data correspond to the last time point (330 h) of the fermentations shown in Fig 5. The average and average deviation of duplicate fermentations are shown for each strain.

Compound	Unit	CBS 12357 ^T	IMS0750
Methanol	mg L ⁻¹	3.3 ± 0.3	3.7 ± 0.3
Propanol	mg L ⁻¹	23.7 ± 2.1	24.1 ± 0.9
Isobutanol	mg L ⁻¹	48.5 ± 2.4	42.9 ± 7.2
Amyl alcohol	mg L ⁻¹	138.5 ± 9.0	155.9 ± 6.4
Diacetyl	µg L ⁻¹	43.8 ± 22.9	7.5 ± 0.2
Ethylacetate	mg L ⁻¹	24.5 ± 5.5	26.1 ± 0.8
Isoamylacetate	mg L ⁻¹	1.4 ± 0.6	3.1 ± 0.3

<https://doi.org/10.1371/journal.pgen.1007853.t001>

transporter which enabled maltotriose uptake [19]. In this study, a 230-bp introgression of *SeMALT3* into the ORF of *SeMALT4* was found, including the 505th and 557th residues. While the shorter α -helices of *SeMALT434* could lead to broader substrate-specificity by increasing structural flexibility, the length of these helices was not affected in *SeMALT413*. As a result, we hypothesize that the acquired maltotriose utilization does not depend solely on specific residues, but rather on the interaction of the residues from the different parental transporters, either by increasing structural flexibility, or by the properties of several critical residues from different α -helices. The 230-bp from *SeMALT3* which were present in *SeMALT413* and in *SeMALT434* may be of particular importance. However, the specific combination of sequences from *SeMALT4*, *SeMALT1* and *SeMALT3* in *SeMALT413* may further contribute to the maltotriose specificity.

Recombinations are an important driver of evolution, as illustrated by the emergence of aerobic growth on citrate during laboratory evolution of *Escherichia coli* [69]. Indeed, a tandem repeat of the citrate/succinate antiporter *citT* placed under the constitutive *rna* promoter enabled aerobic growth on citrate. Moreover, the emergence of a new ORF by recombination has been observed previously between the *TLO* genes of *C. albicans*, although it was not associated with a new gene function [31]. In contrast, the emergence of *SeMALT413* is an example of gene neofunctionalization, which occurred by recombination within genes of the subtelomeric *MALT* family. Neofunctionalization by *in vivo* formation of chimeric sequences is reminiscent of the mechanism used by the pathogen *Trypanosoma brucei* to evade its host's immune system [70]. *T. brucei* expresses a single variant surface glycoprotein (VSG) gene from a subtelomeric location and its genome contains many VSG pseudogenes [71]. Due to 70 bp repetitive elements, the actively expressed VSG gene can be altered by gene conversion from pseudogenes, resulting in a chimeric VSG gene [72–74]. While antigen switching may not qualify as neofunctionalization, it demonstrates the ability of recombinations to diversify gene functions by creating chimeric ORFs. This ability has also been exploited for *in vitro* protein engineering, a strategy known as gene shuffling or gene fusion [75,76]. Gene shuffling involves randomized assembly of diverse DNA sequences into chimeric genes, followed by screening for novel or improved functions. Analogous to *in vitro* gene shuffling, the complex protein remodeling caused by *in vivo* formation of chimeric sequences may be particularly potent for protein neofunctionalization [77]. The demonstration of neofunctionalization of a sugar transporter in *S. eubayanus* by *in vivo* gene shuffling supports the notion that gene fusion is an essential driver of evolution by accelerating the emergence of new enzymatic functions [78]. Moreover, analysis of the *SpMTY1* maltotriose transporter gene revealed a chimeric structure similar to that of *SeMALT413*, albeit with alternating sequence identity with *ScMAL31*, *SeMALT* and *SparMAL31*. While sequences from *S. cerevisiae* and *S. eubayanus* were already present in the genome of *S. pastorianus*, the presence of sequences from *S. paradoxus* is plausible as introgressions from *S. paradoxus* were commonly found in a wide array of *S. cerevisiae* strains [79]. Therefore, the sequence of *SpMTY1* could have resulted from *in vivo* gene shuffling between genes from the *MALT* family, followed by accumulation of mutations. The emergence of *SeMALT413* could therefore be representative of the emergence of maltotriose utilization during the evolution of *S. pastorianus*. Moreover, the emergence of a maltotriose transporter after laboratory evolution of CBS 12357^T, which was discovered at the same time as *SeMALT413* provides further credibility to the evolutionary importance of *in vivo* gene shuffling for gene neofunctionalization [19].

No evidence of reciprocal translocations between *SeMALT1*, *SeMALT3* and *SeMALT4* was found in the genome of IMS0750, indicating genetic introgression via non-conservative recombinations. Such introgressions can occur during repair of double strand breaks by strand invasion of a homologous sequence provided by another chromosome and resection [80],

leading to localized gene conversion and loss of heterozygosity. This model, which was proposed to explain local loss of heterozygosity of two orthologous genes in an *S. cerevisiae* x *S. uvarum* hybrid [80], provides a plausible explanation of the emergence of *SeMALT413* through non-reciprocal recombination between paralogous *SeMALT* genes in *S. eubayanus*. The mosaic sequence composition of the resulting transporter gene suggests that neofunctionalization required multiple successive introgression events. As a result of these genetic introgressions, the *SeMALT4* gene was lost. The fact that IMS0750 harbored two copies of *SeMALT413* and no copy of *SeMALT4* indicates a duplication of the newly-formed ORF at the expense of *SeMALT4* via loss of heterozygosity. As functional-redundancy enables the accumulation of mutation without losing original functions [28,31,32,81], the loss of *SeMALT4* was likely facilitated by the presence of the functionally-redundant maltose transporter *SeMALT2* [9]. The observation that introgressions were only found at *SeMALT4* may be due to the low number of tested mutants. However, it should be noted that introgressions in the *SeMALT1* and *SeMALT3* ORF's would have been unlikely to be beneficial, since these genes are not expressed in CBS 12357^T [9].

This study illustrates the role of the rapid evolution of subtelomeric genes in adaptation to environmental changes. In *Saccharomyces* yeasts, subtelomeric regions contain a large number of gene families encoding functions critical to the interaction of a cell with its environment, such as nutrient uptake, sugar utilization, inhibitor tolerance and flocculation [28,82–87]. The high number of genes within subtelomeric families results in functional redundancy and therefore in mutational freedom [28,31,32,81]. In *Saccharomyces* species, many industrially-relevant brewing traits are encoded by subtelomeric gene families, such as the *MAL* genes encoding maltose utilization and the *FLO* genes encoding flocculation [88]. While subtelomeric regions are difficult to reconstruct due to their repetitive nature, they encode much of the genetic diversity between genomes [89,90]. *A posteriori* sequence analysis of existing gene families can elucidate their evolutionary history. For example, the α -glucosidase genes from the *MALS* family emerged by expansion of an ancestral pre-duplication gene with maltose-hydrolase activity and trace isomaltose-hydrolase activity [15]. The evolution of *MALS* isomaltase genes from this ancestral gene is an example of subfunctionalization: the divergent evolution of two gene copies culminating in their specialization for distinct functions which were previously present to a lesser extent in the ancestral gene. The generation of functional redundancy by gene duplication is critical to this process as it enables mutations to occur which result in loss of the original gene function without engendering a selective disadvantage [28,31,32,36,37,81]. In contrast to subfunctionalization, neofunctionalization consists of the emergence of a function which was completely absent in the ancestral gene [40]. While the emergence of many genes from a large array of organisms has been ascribed to subfunctionalization and to neofunctionalization, these conclusions were based on *a posteriori* analysis of processes which had already occurred, and not on their experimental observation [15,28,31,39–42]. *Ex-vivo* engineering of the subtelomeric *FLO* genes demonstrated that recombinations within subtelomeric gene families can alter their function [39]. However, *in vivo* neofunctionalization within a subtelomeric gene family was never observed in real time. Here we present clear experimental evidence of neofunctionalization within a laboratory evolution experiment. The ability of *SeMALT413* to transport maltotriose proves that such *in vivo* gene shuffling is relevant for evolutionary biology. Given their high genetic redundancy of subtelomeric gene families, and the large body of evidence of gene sub- and neofunctionalization in their evolutionary history, it is likely that subtelomeric localization of genes facilitates the emergence of new functions. As a result, subtelomeric regions would not only be a hotspot of genetic diversity between different genomes, but also a preferred location for the birth of new genes and new gene functions.

While *SeMALT413* was shown to enable maltotriose utilization, it remained unclear how the UV-mutagenized cells acquired the ability to utilize maltotriose and why these mutations were insufficient to enable maltotriose utilization in wort. Since maltotriose-consuming mutants did not arise in the absence of UV-mutagenesis, the ability to utilize maltotriose likely emerged as a result of genetic evolution rather than due to epigenetic adaptation. Moreover, the introduction of *SeMALT413* in CBS 12357^T resulted in slower maltotriose utilization than IMS0750, suggesting that other mutations may contribute to the maltotriose-utilization phenotype of IMS0750. While whole genome sequencing of IMS0637-IMS0643 revealed a wide array of mutations, none affected genes which were previously linked to maltotriose utilization. The fact that *SeMALT1*, *SeMALT2*, *SeMALT3* and *SeMALT4* could be PCR amplified from the IMS0637 genome while *SeMALT413* could not, indicates that maltotriose utilization was not due to an undetected *SeMALT413* gene. In addition, alignment of short-read data to the reference genome and *de novo* genome assembly based on long-read data did not reveal any mutations affecting *MAL* genes, except a recombination between CHRII and CHRVII, which resulted in the loss of one of the two copies of *SeMALT1*. Since deletion of *SeMALT1* does not enable maltotriose utilization in CBS 12357^T [9], this mutation is unlikely to be causal. While one of the 122 mutations affecting the UV-mutagenized strains or additional undetected mutations may have contributed to maltotriose utilization, their elucidation is beyond the scope of this study. Moreover, while overexpression of *SeMALT413* in CBS 12357^T resulted in lesser maltotriose utilization than the evolved strain IMS0750, the maltotriose transporter *SeMalT413* is not necessarily suboptimal. Indeed, when overexpressing transporters suboptimal growth is commonly observed and has been attributed to imbalances between transporter activity and the subsequent metabolic steps [91,92]. Overall, regardless of the presence of other mutations contributing to maltotriose utilization, the emergence of the maltotriose transporter gene *SeMAL413* from parental genes which do not enable maltotriose transport demonstrates that gene neofunctionalization occurred.

While the introduction of *SeMALT413* in CBS 12357^T via genetic engineering demonstrated its neofunctionalization, the use of GMO-strains is limited in the brewing industry by customer acceptance issues [93]. However, the non-GMO evolved *S. eubayanus* isolate IMS0750 could be tested on industrial brewing wort at 7 L scale. In addition to near-complete maltotriose conversion, the maltose consumption, isoamylacetate production and diacetyl degradation of IMS0750 were superior to CBS 12357^T. While the increased maltotriose consumption could be at least partially attributed to the emergence of the *SeMALT413*, it remained unclear if and what mutations could underlay the other changes. However, efficient maltose and maltotriose consumption, as well as the concomitantly increased ethanol production, are important factors determining the economic profitability of beer brewing processes [94]. In addition, low residual sugar concentration, low concentrations of diacetyl and high concentrations of isoamylacetate are desirable for the flavor profile of beer [95,96]. *S. eubayanus* strains typically generate high concentrations of 4-vinyl guaiacol, a clove-like off-flavor [97,98], a strategy to eliminate this production in *S. eubayanus* have recently been described [97]. Therefore, expansion of phenotypic landscape of *S. eubayanus* might be accelerated by combining these domesticated traits. In terms of application, the laboratory evolution approach for conferring maltotriose utilization into *S. eubayanus* presented in this paper is highly relevant in view of the recent introduction of this species in industrial-scale brewing processes [9,99]. The ability to ferment maltotriose can be introduced into other natural isolates of *S. eubayanus*, either by laboratory evolution or by crossing with evolved strains such as *S. eubayanus* IMS0750. Besides their direct application for brewing, maltotriose-consuming *S. eubayanus* strains are of value for the generation of laboratory-made hybrid *Saccharomyces* strains for brewing and other industrial applications [8,100–102].

Materials and methods

Strains and maintenance

All yeast strains used and generated in this study are listed in Table 2. *S. eubayanus* type strain CBS 12357^T [1] and *S. pastorianus* strain CBS 1483 [55,103] were obtained from the Westerdijk Fungal Biodiversity Institute (Utrecht, the Netherlands). Stock cultures were grown in YPD, containing 10 g L⁻¹ yeast extract, 20 g L⁻¹ peptone and 20 g L⁻¹ glucose, at 20°C until late exponential phase, complemented with sterile glycerol to a final concentration of 30% (v/v) and stored at -80°C until further use.

Media and cultivation

Plasmids were propagated overnight in *Escherichia coli* XL1-Blue cells in 10 mL LB medium containing 10 g L⁻¹ peptone, 5 g L⁻¹ Bacto Yeast extract, 5 g L⁻¹ NaCl and 100 mg L⁻¹ ampicillin at 37°C. YPD medium was prepared using 10 g L⁻¹ yeast extract, 20 g L⁻¹ peptone and 20 g L⁻¹ glucose. Synthetic medium (SM) contained 3.0 g L⁻¹ KH₂PO₄, 5.0 g L⁻¹ (NH₄)₂SO₄, 0.5 g L⁻¹ MgSO₄, 7 H₂O, 1 mL L⁻¹ trace element solution, and 1 mL L⁻¹ vitamin solution [56], and was supplemented with 20 g L⁻¹ glucose (SMG), maltose (SMM) or maltotriose (SMMt) by addition of autoclaved 50% w/v sugar solutions. Maltotriose (95.8% purity) was obtained from Glentham Life Sciences, Corsham, United Kingdom. Industrial wort was provided by HEINEKEN Supply Chain B.V., Zoeterwoude, the Netherlands. The wort was supplemented with 1.5 mg L⁻¹ of Zn²⁺ by addition of ZnSO₄·7H₂O, autoclaved for 30 min at 121°C and filtered using Nalgene 0.2 μm SFCA bottle top filters (Thermo Scientific, Waltham, MA) prior to use. Where indicated, filtered wort was diluted with sterile demineralized water. Solid media were supplemented with 20 g L⁻¹ of Bacto agar (Becton Dickinson, Breda, The Netherlands). *S. eubayanus* strains transformed with plasmids pUDP052 (gRNA_{SeSGA1}) were selected on medium in which (NH₄)₂SO₄ was replaced by 5 g L⁻¹ K₂SO₄ and 10 mM acetamide (SM_{AccG}) [104].

Shake-flask cultivation. Shake-flask cultures were grown in 500 mL shake flasks containing 100 mL medium and inoculated from stationary-phase aerobic precultures to an initial OD₆₆₀ of 0.1. Inocula for growth experiments on SMMt were grown on SMM. In other cases, media for growth experiments and inoculum preparation were the same. Shake flasks were incubated at 20°C and 200 RPM in a New Brunswick Innova43/43R shaker (Eppendorf)

Table 2. *Saccharomyces* strains used during this study.

Name	Species	Relevant genotype	Origin
CBS 12357	<i>S. eubayanus</i>	Wild-type diploid	[1]
IMS0637	<i>S. eubayanus</i>	Evolved strain derived from CBS 12357	This study
IMS0638	<i>S. eubayanus</i>	Evolved strain derived from CBS 12357	This study
IMS0639	<i>S. eubayanus</i>	Evolved strain derived from CBS 12357	This study
IMS0640	<i>S. eubayanus</i>	Evolved strain derived from CBS 12357	This study
IMS0641	<i>S. eubayanus</i>	Evolved strain derived from CBS 12357	This study
IMS0642	<i>S. eubayanus</i>	Evolved strain derived from CBS 12357	This study
IMS0643	<i>S. eubayanus</i>	Evolved strain derived from CBS 12357	This study
IMS0750	<i>S. eubayanus</i>	Evolved strain derived from CBS 12357	This study
IMS0751	<i>S. eubayanus</i>	Evolved strain derived from CBS 12357	This study
IMS0752	<i>S. eubayanus</i>	Evolved strain derived from CBS 12357	This study
IMX1941	<i>S. eubayanus</i>	Δ <i>Sesga1</i> :: <i>ScTEF1_p</i> - <i>SeMALT2</i> - <i>ScCYC1_t</i>	This study
IMX1942	<i>S. eubayanus</i>	Δ <i>Sesga1</i> :: <i>ScTEF1_p</i> - <i>SeMALT413</i> - <i>ScCYC1_t</i>	This study
CBS 1483	<i>S. pastorianus</i>	Group II brewer's yeast, Brewery Heineken, bottom yeast, July 1927	[103]

<https://doi.org/10.1371/journal.pgen.1007853.t002>

Nederland B.V., Nijmegen, The Netherlands). Samples were taken at regular intervals to determine OD₆₆₀ and extracellular metabolite concentrations. OD₆₆₀ measurements were taken with a Jenway 7200 spectrometer (Cole-Parmer, Staffordshire, UK) unless indicated otherwise.

Microaerobic growth experiments. Microaerobic cultivation was performed in 250 mL airlock-capped Neubor infusion bottles (38 mm neck, Dijkstra, Lelystad, Netherlands) containing 200 mL 3-fold diluted wort supplemented with 0.4 mL L⁻¹ Pluronic antifoam (Sigma-Aldrich). Bottle caps were equipped with a 0.5 mm x 16 mm Microlance needle (BD Biosciences) sealed with cotton to prevent pressure build-up. Sampling was performed aseptically with 3.5 mL syringes using a 0.8 mm x 50 mm Microlance needle (BD Biosciences). Microaerobic cultures were inoculated at an OD₆₆₀ of 0.1 from stationary-phase precultures in 50 mL Bio-One Cellstar Cellreactor tubes (Sigma-Aldrich) containing 30 mL of the same medium, grown for 4 days at 12°C. Bottles were incubated at 12°C and shaken at 200 RPM in a New Brunswick Innova43/43R shaker. At regular intervals, 3.5 mL samples were collected in 24 deep-well plates (EnzyScreen BV, Heemstede, Netherlands) using a LiHa liquid handler (Tecan, Männedorf, Switzerland) to measure OD₆₆₀ and external metabolites. 30 µL of each sample was diluted 5 fold in demineralized water in a 96 well plate and OD₆₆₀ was measured with a Magellan Infinite 200 PRO spectrophotometer (Tecan, Männedorf, Switzerland). From the remaining sample, 150 µL was vacuum filter sterilized using 0.2 µm Multiscreen filter plates (Merck, Darmstadt, Germany) for HPLC measurements.

7 L wort fermentation cultivations. Batch cultivations under industrial conditions were performed in 10 L stirred stainless-steel fermenters containing 7 L of 16.6° Plato wort. Fermentations were inoculated to a density of 5 x 10⁶ cells mL⁻¹ at 8°C. The temperature was raised during 48 hours to 11°C and increased to 14°C as soon as the gravity was reduced to 6.5° Plato. Samples were taken daily during weekdays and the specific gravity and alcohol content were measured using an Anton Paar density meter (Anton Paar GmbH, Graz, Austria).

Adaptive laboratory evolution

UV-mutagenesis and selection. First, we attempted to obtain maltotriose-consuming mutants without UV-mutagenesis. To this end, *S. eubayanus* CBS 12357^T was grown in a 500 mL shake flask containing 100 mL SMG at 20°C until stationary phase. Cells were washed twice with demineralized water and used to inoculate a 50 mL shake flask containing 10 mL SMMt to an OD₆₆₀ of 2, corresponding to an initial inoculum of approximately 10⁸ cells. The SMMt culture was incubated at 20°C and 200 RPM during three months. During this period, no growth was observed and HPLC measurements did not show any maltotriose consumption after three months.

In parallel, we mutagenized spores of *S. eubayanus* CBS 12357^T to increase the likelihood of beneficial mutations. To this end, *S. eubayanus* CBS 12357^T was grown in a 500 mL shake flask containing 100 mL SMG at 20°C until stationary phase. The resulting cells were washed twice with demineralized water and transferred to a 500 mL shake flask containing 100 mL of 20 g/L potassium acetate at pH 7.0 to sporulated. After three days, the presence of ascospores was verified by optic microscopy and diluted to an OD₆₆₀ of 1. Of the resulting suspension, 50 mL was spun down at 4816 g for 5 min and washed twice with demineralized water. 25 mL of washed cells was poured into a 100 mm x 15 mm petri dish (Sigma-Aldrich) without lid and irradiated with a UV lamp (TUV 30 W T8, Philips, Eindhoven, The Netherlands) at a radiation peak of 253.7 nm. 25 mL of non-mutagenized and 5 mL of mutagenized cells were kept to determine survival rate. From both samples, a 100-fold dilution was made, from which successive 10-fold dilutions were made down to a 100,000-fold dilution. Then, 100 µL of each dilution was plated on YPD agar and the number of colonies were counted after incubation during 48h at room

temperatures. After 10,000-fold dilution, 182 colonies formed from the non-mutagenized cells against 84 colonies for the mutagenized cells, indicating a survival rate of 46%. The remaining 20 mL of mutagenized cells, corresponding to about 10^{+8} cells, was spun down at 4816 g for 5 min and resuspended in 1 mL demineralized water. These mutagenized cells were added to a 50 mL shake flask containing 9 mL SMMt and incubated for 21 days at 20°C and 200 RPM. Maltotriose concentrations were analyzed at day 0, 19 and 21. After 21 days, two 100 μ L samples were transferred to fresh shake flasks containing SMMt and incubated until stationary phase. At the end of the second transfer, single cell isolates were obtained using the BD FACSAria II SORP Cell Sorter (BD Biosciences, Franklin Lakes, NJ) equipped with a 488 nm laser and a 70 μ m nozzle, and operated with filtered FACSFlow (BD Biosciences). Cytometer performance was evaluated by running a CST cycle with CS&T Beads (BD Biosciences). Drop delay for sorting was determined by running an Auto Drop Delay cycle with Accudrop Beads (BD Biosciences). Cell morphology was analysed by plotting forward scatter (FSC) against side scatter (SSC). Gated single cells were sorted into a 96 well microtiter plates containing SMMt using a “single cell” sorting mask, corresponding to a yield mask of 0, a purity mask of 32 and a phase mask of 16. The 96 well plates were incubated for 96 h at room temperature in a GENios Pro micro plate spectrophotometer (Tecan, Männedorf, Switzerland), during which period growth was monitored as OD₆₆₀. After 96 h, biomass in each well was resuspended using a sterile pin replicator and the final OD₆₆₀ was measured. The 7 isolates with the highest final OD₆₆₀ were picked, restreaked and stocked as isolates IMS0637-643. PCR amplification of the *S. eubayanus*-specific *SeFSY1* gene and ITS sequencing confirmed that all 7 isolates were *S. eubayanus*.

Laboratory evolution in chemostats. Chemostat cultivation was performed in Multifors 2 Mini Fermenters (INFORS HT, Velp, The Netherlands) equipped with a level sensor to maintain a constant working volume of 100 mL. The culture temperature was controlled at 20°C and the dilution rate was set at 0.03 h⁻¹ by controlling the medium inflow rate. Cultures were grown on 6-fold diluted wort supplemented with 10 g L⁻¹ additional maltotriose (Glenham Life Sciences), 0.2 mL L⁻¹ anti-foam emulsion C (Sigma-Aldrich), 10 mg L⁻¹ ergosterol, 420 mg L⁻¹ Tween 80 and 5 g L⁻¹ ammonium sulfate. Tween 80 and ergosterol were added as a solution as described previously [56]. IMS0637-IMS0643 were grown overnight at 20°C and 200 RPM in separate shake flasks on 3-fold diluted wort. The OD₆₆₀ of each strain was measured and the equivalent of 7 mL at an OD₆₆₀ of 20 from each strain was pooled in a total volume of 50 mL. The reactor was inoculated by adding 20 mL of the pooled culture. After overnight growth, the medium inflow pumps were turned on and the fermenter was sparged with 20 mL min⁻¹ of nitrogen gas and stirred at 500 RPM. The pH was not adjusted. Samples were taken weekly. Due to a technical failure on the 63rd day, the chemostat was autoclaved, cleaned and restarted using a sample taken on the same day. After a total of 122 days, the chemostat was stopped and 10 single colony isolates were sorted onto SMMt agar using FACS, as for IMS0637-IMS0643. PCR amplification of the *S. eubayanus* specific *SeFSY1* gene and ITS sequencing confirmed that all ten single-cell isolates were *S. eubayanus*. Three colonies were randomly picked, restreaked and stocked as IMS0750-752.

Genomic isolation and whole genome sequencing. Yeast cultures were incubated in 50 mL Bio-One Cellstar Cellreactor tubes (Sigma-Aldrich) containing liquid YPD medium at 20°C on an orbital shaker set at 200 RPM until the strains reached stationary phase with an OD₆₆₀ between 12 and 20. Genomic DNA for whole genome sequencing was isolated using the Qiagen 100/G kit (Qiagen, Hilden, Germany) according to the manufacturer’s instructions and quantified using a Qubit Fluorometer 2.0 (Thermo Scientific).

Genomic DNA of the strains CBS 12357^T and IMS0637-IMS0643 was sequenced by Novogene Bioinformatics Technology Co., Ltd (Yuen Long, Hong Kong) on a HiSeq2500 sequencer

(Illumina, San Diego, CA) with 150 bp paired-end reads using PCR-free library preparation. Genomic DNA of the strains IMS0750 and IMS0752 was sequenced in house on a MiSeq sequencer (Illumina) with 300 bp paired-end reads using PCR-free library preparation. All reads are available at NCBI (<https://www.ncbi.nlm.nih.gov/>) under the bioproject accession number PRJNA492251.

Genomic DNA of strains IMS0637 and IMS0750 was sequenced on a Nanopore MinION (Oxford Nanopore Technologies, Oxford, United Kingdom). Libraries were prepared using 1D-ligation (SQK-LSK108) as described previously [90] and analysed on FLO-MIN106 (R9.4) flow cell connected to a MinION Mk1B unit (Oxford Nanopore Technology). MinKNOW software (version 1.5.12; Oxford Nanopore Technology) was used for quality control of active pores and for sequencing. Raw files generated by MinKNOW were base called using Albacore (version 1.1.0; Oxford Nanopore Technology). Reads with a minimum length of 1000 bp were extracted in fastq format. All reads are available at NCBI (<https://www.ncbi.nlm.nih.gov/>) under the bioproject accession number PRJNA492251.

Genome analysis. For the strains CBS 12357^T, IMS0637-IMS0643, IMS0750 and IMS0752, the raw Illumina reads were aligned against a chromosome-level reference genome of CBS 12357^T (NCBI accession number PRJNA450912, <https://www.ncbi.nlm.nih.gov/>) [9] using the Burrows–Wheeler Alignment tool (BWA), and further processed using SAMtools and Pilon for variant calling [105–107]. Heterozygous SNPs and INDELS which were heterozygous in CBS 12357^T were disregarded. Chromosomal translocations were detected using Breakdancer [108]. Only translocations which were supported by at least 10% of the reads aligned at that locus were considered. Chromosomal copy number variation was estimated using Magnolya [109] with the gamma setting set to “none” and using the assembler ABySS (v 1.3.7) with a k-mer size of 29 [110]. All SNPs, INDELS, recombinations and copy number changes were manually confirmed by visualising the generated .bam files in the Integrative Genomics Viewer (IGV) software [111]. The complete list of identified mutations can be found in [S1 Data File](#).

For strains IMS0637 and IMS0750, the nanopore sequencing reads were assembled *de novo* using Canu (version 1.3) [112] with–genomesize set to 12 Mbp. Assembly correctness was assessed using Pilon [107], and sequencing/assembly errors were polished by aligning Illumina reads with BWA [105] using correction of only SNPs and short indels (–fix bases parameter). Long sequencing reads of IMS0637 and IMS0750 were aligned to the obtained reference genomes and to the reference genome of CBS 12357^T using minimap2 [113]. The genome assemblies for IMS0637 and IMS0750 are available at NCBI (<https://www.ncbi.nlm.nih.gov/>) under the bioproject accession number PRJNA492251.

Molecular biology methods. For colony PCR and Sanger sequencing, a suspension containing genomic DNA was prepared by boiling biomass from a colony in 10 µL 0.02 M NaOH for 5 min, and spinning cell debris down at 13,000 g. To verify isolates belonged to the *S. eubayanus* species, the presence of *S. eubayanus*-specific gene *SeFSY1* and the absence of *S. cerevisiae*-specific gene *ScMEX67* was tested by DreamTaq PCR (Thermo Scientific) amplification using primer pair 8572/8573 [114], and primer pair 8570/8571 [115], respectively. Samples were loaded on a 1% agarose gel containing SYBR Green DNA stain (Thermo Scientific). GeneRuler DNA Ladder Mix (Thermo Scientific) was used as ladder and gel was run at a constant 100V for 20 min. DNA bands were visualized using UV light. For additional confirmation of the *S. eubayanus* identity, ITS regions were amplified using Phusion High-Fidelity DNA polymerase (Thermo Scientific) and primer pair 10199/10202. The purified (GenElute PCR Cleanup Kit, Sigma-Aldrich) amplified fragments were Sanger sequenced (BaseClear, Leiden, Netherlands) [116]. Resulting sequences were compared using BLAST to available ITS sequences of *Saccharomyces* species and classified as the species to which the amplified region

had the highest sequence identity. The presence of the *SeMALT* genes was verified by using Phusion High-Fidelity DNA polymerase and gene specific primers: 10491/10492 for *SeMALT1*, 10632/10633 for *SeMALT2* and *SeMALT4/2*, 10671/10672 for *SeMALT3*, 10491/10671 for *SeMALT13*, and 10633/10671 for *SeMALT413*. The amplified fragments were purified using the GenElute PCR Cleanup Kit (Sigma-Aldrich) and Sanger sequenced (BaseClear) using the same primers used for amplification.

Plasmid construction. All plasmids and primers used in this study are listed in Table 3 and S1 Table, respectively. DNA amplification for plasmid and strain construction was performed using Phusion High-Fidelity DNA polymerase (Thermo Scientific) according to the supplier's instructions. The coding region of *SeMALT413* was amplified from genomic DNA of IMS0750 with primer pair 10633/10671. Each primer carried a 40 bp extension complementary to the plasmid backbone of p426-TEF-amdS [16], which was PCR amplified using primer pair 7812/5921. The transporter fragment and the p426-TEF-amdS backbone fragment were assembled [117] using NEBuilder HiFi DNA Assembly (New England Biolabs, Ipswich, MA), resulting in plasmid pUD814. The resulting pUD814 plasmid was verified by Sanger sequencing, which confirmed that its *SeMALT413* ORF was identical to the recombined ORF found in the nanopore assembly of IMS0750 (Fig 3C).

Strain construction. To integrate and overexpress *SeMALT2* and *SeMALT413* ORFs in *S. eubayanus* CBS 12357^T, *SeMALT2* and *SeMALT413* were amplified from pUD480 and pUD814 respectively with primers 13559/13560 that carried a 40 bp region homologous to each flank of the *SeSGA1* gene located on *S. eubayanus* chromosome IX. To facilitate integration, the PCR fragments were co-transformed with the plasmid pUDP052 that expressed *SpCas9*^{D147Y P411T} [119,120] and a gRNA targeting *SeSGA1* [9]. The strain IMX1941 was constructed by transforming CBS 12357^T with 1 µg of the amplified *SeMALT2* expression cassette and 500 ng of plasmid pUDP052 by electroporation as described previously [120]. Transformants were selected on SM_{Acc}-G plates. Similarly, IMX1942 was constructed by transforming CBS 12357^T with 1 µg of the amplified *SeMALT413* expression cassette for *SeMALT413* instead of *SeMALT2*. Correct integration was verified by diagnostic PCR with primer pair 12635/12636 (S9 Fig). All PCR-amplified gene sequences were Sanger sequenced (BaseClear).

Protein structure prediction. Homology modeling of the *SeMalT413* transporter was performed using the SWISS-MODEL server (<https://swissmodel.expasy.org/>) [121]. The translated amino acid sequence of *SeMALT413* was used as input (S4 Fig). The model of the xylose proton symporter XylE (PDB: 4GBY) was chosen as template [57]. Models were built based on the target-template alignment using ProMod3. Coordinates which are conserved between the target and the template are copied from the template to the model. Insertions and deletions are remodeled using a fragment library. Side chains are then rebuilt. Finally, the geometry of the

Table 3. Plasmids used during this study.

Name	Relevant genotype	Source
pUDP052	<i>ori</i> (ColE1) <i>bla</i> panARSopt <i>amdSYM</i> <i>ScTDH3</i> _p -gRNA _{SeSGA1} - <i>ScCYC1</i> _t <i>AaTEF1</i> _p - <i>SpCas9</i> ^{D147Y P411T} - <i>ScPHO5</i> _t	[9]
pUDE044	<i>ori</i> (ColE1) <i>bla</i> 2µ <i>ScTDH3</i> _p - <i>ScMAL12</i> - <i>ScADH1</i> _t <i>URA3</i>	[118]
p426-TEF-amdS	<i>ori</i> (ColE1) <i>bla</i> 2µ <i>amdSYM</i> <i>ScTEF1</i> _p - <i>ScCYC1</i> _t	[16]
pUD479	<i>ori</i> (ColE1) <i>bla</i> 2µ <i>amdSYM</i> <i>ScTEF1</i> _p - <i>SeMALT1</i> - <i>ScCYC1</i> _t	[9]
pUD480	<i>ori</i> (ColE1) <i>bla</i> 2µ <i>amdSYM</i> <i>ScTEF1</i> _p - <i>SeMALT2</i> - <i>ScCYC1</i> _t	[9]
pUD814	<i>ori</i> (ColE1) <i>bla</i> 2µ <i>amdSYM</i> <i>ScTEF1</i> _p - <i>SeMALT413</i> - <i>ScCYC1</i> _t	This study

<https://doi.org/10.1371/journal.pgen.1007853.t003>

resulting model is regularized by using a force field. In case loop modelling with ProMod3 fails, an alternative model is built with PROMOD-II [122]. 3D model was assessed and colored using Pymol (The PyMOL Molecular Graphics System, Version 2.1.1 Schrödinger, LLC.).

Sequence analysis of *SpMTY1*. The sequence of *SpMTY1* was analyzed by aligning *ScMAL31*, *ScAGT1*, *ScMPH2* and *ScMPH3* from *S. cerevisiae* strain S288C (63) and *SeMALT1*, *SeMALT2*, *SeMALT3*, *SeMALT4* from *S. eubayanus* strain CBS 12357^T [9] to the sequence of *SpMTY1* from *S. pastorianus* strain Weihenstephan 34/70 [21] using the Clone manager software (version 9.51, Sci-Ed Software, Denver, Colorado). The origin of nucleotides 969 to 1,639 of *SpMTY1* was further investigated using the blastn function of NCBI (<https://www.ncbi.nlm.nih.gov/>). The sequence was aligned against *S. cerevisiae* S288C (taxid:559292) to identify closely related homologues. In addition, *SpMTY1* was aligned against the complete nucleotide collection. To avoid matches with genomes harboring an *MTY1* gene, sequences from *S. pastorianus* (taxid:27292), *S. cerevisiae* (taxid:4932), *S. eubayanus* (taxid:1080349), *S. cerevisiae* x *eubayanus* (taxid:1684324) and *S. bayanus* (taxid:4931) were excluded. The most significant alignment was with nucleotides 1,043,930 to 1,044,600 of chromosome VII of *S. paradoxus* strain YPS138 (GenBank: CP020282.1). As the most significant alignment of these nucleotides to *S. cerevisiae* S288C (taxid:559292) was *ScMAL31*, the gene was further referred to as *SparMAL31*.

Analytics. The concentrations of ethanol and of the sugars glucose, maltose and maltotriose were measured using a high pressure liquid chromatography (HPLC) Agilent Infinity 1260 series (Agilent Technologies, Santa Clara, CA) using a Bio-Rad Aminex HPX-87H column at 65°C and a mobile phase of 5 mM sulfuric acid with a flow rate of 0.8 mL per minute. Compounds were measured using a RID at 35°C. Samples were spun down (13,000 g for 5 min) to collect supernatant or 0.2 µm filter-sterilized before analysis. The concentrations of ethylacetate and isoamylacetate, methanol, propanol, isobutanol, isoamyl alcohol and diacetyl were determined as described previously [55].

Supporting information

S1 Table. Primers used in this study.

(DOCX)

S1 Fig. Characterization of enriched mutants IMS0637-IMS0643 on SMMt. Characterization of *S. pastorianus* CBS 1483 (black), *S. eubayanus* CBS 12357^T (blue) and selected mutants IMS0637-IMS0643 (light red) on SMMt at 20°C. The average concentration of maltotriose (diamonds) and average deviation were determined from two replicates. IMS0637 was chosen as representative for all mutants (S8 Data File).

(TIF)

S2 Fig. Growth curves for the strains CBS 1483 (squares), CBS 12357^T, (upward triangles), IMS0750 (downward triangles), IMS0751 (diamonds) and IMS0752 (circles) on 3x diluted wort at 12°C. (A) Consumption of glucose, (B) maltose, (C) maltotriose and (D) ethanol were measured by HPLC. Data represent average and standard deviation of three biological replicates (S9 Data File).

(TIF)

S3 Fig. Sequence alignment of the *SeMALT* transporter genes from CBS 12357^T to the new recombined *SeMALT413* transporter gene from IMS0750. The alignment was performed using the Clone manager software (version 9.51, Sci-Ed Software). Identical nucleotides are shown by dots and nucleotides which differ from *SpMTY1* are shown in orange. In addition, the sequences which match exactly are highlighted in yellow for *SeMALT4*, in green for

SeMALT1 and in blue for *SeMALT3*.
(TIF)

S4 Fig. Alignment of SeMalt413 to XylE using by ProMod3 for protein structure prediction. Transmembrane domain α -helices are indicated in red.
(TIF)

S5 Fig. Protein structure overlay of SeMalt1 (green), SeMalt4 (orange), SeMalt3 (blue) and SeMalt413 (magenta). *SeMALT* genes were translated into amino acid sequence and used for structural prediction using SWISS-MODEL with XylE as a structural template. Resulting SeMalt protein structures were overlaid using PyMOL.
(TIF)

S6 Fig. Amplification of the SeSGA1 locus to verify integration of SeMALT2 in IMX1941 and of SeMALT413 in IMX1942. The *SeSGA1* locus was amplified from genomic DNA of IMX1941 (1), IMX1942 (2) and CBS 12357^T (3) using primers 12635/12636 and Phusion polymerase (Thermo Fischer Scientific). At the *SeSGA1* locus, IMX1941 should harbor *ScTEF1p-SeMALT2-ScCYC1t* and IMX1942 should harbor *ScTEF1p-SeMALT413-ScCYC1t*. As a negative control, a PCR was done with primers 12635/12636 without template DNA. L indicates the GeneRuler DNA Ladder Mix (Thermo Fischer Scientific).
(TIF)

S7 Fig. Characterization of CBS 12357^T (blue squares), IMS0750 (red triangles), IMX1941 (cyan triangles), IMX1942 (purple diamonds) on SM (A) glucose, (B) maltose and (C) maltotriose. Strains were cultivated at 20°C and optical densities were measured at 660 nm. Data represent average and standard deviation of three biological replicates (S10 Data File). Blue boxes represent the timeframe used to calculate growth rates.
(TIF)

S8 Fig. Alignment of ScMAL31, SeMALT3 and SparMAL31 to SpMTY1 as obtained using Clone Manager. Identical nucleotides are shown by dots and nucleotides which differ from *SpMTY1* are shown in orange. In addition, the high-identity sequences described in the main text are highlighted in yellow for *ScMAL31*, in green for *SeMALT3* and in blue for *SparMAL31*.
(TIF)

S9 Fig. PCR amplification of SeMALT genes in wild type CBS 12357^T and evolved mutant IMS0750. The *SeMALT* genes were amplified from genomic DNA of CBS 12357^T and IMS0750 using Phusion polymerase (Thermo Fischer Scientific). Lanes show PCR products for *SeMALT1* (primers 10491/10492), *SeMALT2* and *SeMALT4* (primers 10633/10632), *SeMALT3* (primers 10672/10671) and *SeMALT413* (primers 10633/10671). As a negative control, a PCR was done with primers 10633/10632 without template DNA. L indicates the GeneRuler DNA Ladder Mix (Thermo Fischer Scientific).
(TIF)

S1 Data. Overview of all mutations identified in the mutagenized strains IMS0637-IMS0643 and in the evolved strains IMS0750-IMS0752. The mutations were obtained using Pilon by alignment against the chromosome level assembly of *S. eubayanus* strain CBS12357. The mutations are ordered per strain, and for each mutation, the strains in which the same mutation is found are indicated. SNP indicates single nucleotide polymorphisms, INDELS indicate small insertions and deletions and CNV indicates copy number variation. NON indicates a premature stop codon, NSY indicates a non-synonymous mutation and SYN a

synonymous mutation.
(XLSX)

S2 Data. Belonging to Fig 2A. Characterization of *S. pastorianus* CBS 1483, *S. eubayanus* CBS 12357 and IMS0637-0643 on SMMt at 20°C. Maltotriose concentrations were measured for two biological replicates using HPLC.

(XLSX)

S3 Data. Belonging to Fig 2B. Characterization of *S. pastorianus* CBS 1483, *S. eubayanus* CBS 12357 and IMS0637-0643 on wort at 20°C. Concentrations of glucose, maltose and maltotriose were measured from single biological samples using HPLC.

(XLSX)

S4 Data. Belonging to Fig 2C. Residual maltotriose concentration in the outflow during laboratory evolution of strains IMS0637-IMS0643 in an anaerobic chemostat at 20°C on maltotriose enriched wort. The concentrations of glucose, maltose and maltotriose were measured from a single chemostat by HPLC.

(XLSX)

S5 Data. Belonging to Fig 2D. Characterization of *S. pastorianus* CBS 1483, *S. eubayanus* CBS 12357 and IMS0750 on wort at 12°C. Glucose, maltose and maltotriose concentrations were determined from three biological replicates with HPLC.

(XLSX)

S6 Data. Belonging to Fig 4B. Characterization of CBS 12357, IMS0750, IMX1941, IMX1942 on SM glucose, maltose and maltotriose. Strains were cultivated at 20°C and culture supernatant was measured from three biological replicates using HPLC.

(XLSX)

S7 Data. Belonging to Fig 5. Extracellular metabolite profiles of *S. eubayanus* strains CBS 12357 and IMS0750 in high-gravity wort at 7 L pilot scale. Fermentations were performed on wort with a gravity of 16.6° Plato. The concentrations of glucose, maltose, maltotriose and ethanol were measured from two biological replicates using HPLC.

(XLSX)

S8 Data. Belonging to S1 Fig. Characterization of enriched mutants IMS0637-IMS0643 on SMMt at 20°C. Concentrations of maltotriose were measured from two biological replicates using HPLC.

(XLSX)

S9 Data. Belonging to S2 Fig. Growth curves for the strains CBS 1483 CBS 12357, IMS0750, IMS0751 and IMS0752 on 3x diluted wort at 12°C. Concentrations of glucose, maltose, maltotriose and ethanol were measured from three biological replicates using HPLC.

(XLSX)

S10 Data. Belonging to S7 Fig. Characterization of CBS 12357, IMS0750, IMX1941, IMX1942 on SM glucose, maltose and maltotriose. Strains were cultivated at 20°C and optical densities were measured from three biological replicates at 660 nm.

(XLSX)

Acknowledgments

We thank Jan-Maarten Geertman (Heineken Supply Chain B.V.) for his support during the study. We are grateful to Dr. EmilyClare Baker and Dr. Chris Todd Hittinger for delaying the

public release of the non-copy-edited version of their work during the revision process of our manuscript. A pre-print version of this article has been uploaded on bioRxiv (DOI: [10.1101/428839](https://doi.org/10.1101/428839)) [123].

Author Contributions

Conceptualization: Nick Brouwers, Arthur R. Gorter de Vries, Jack T. Pronk, Jean-Marc G. Daran.

Data curation: Nick Brouwers, Arthur R. Gorter de Vries, Marcel van den Broek.

Formal analysis: Nick Brouwers, Arthur R. Gorter de Vries, Marcel van den Broek.

Funding acquisition: Jean-Marc G. Daran.

Investigation: Nick Brouwers, Arthur R. Gorter de Vries, Susan M. Weening, Tom D. Elink Schuurman.

Project administration: Jean-Marc G. Daran.

Software: Marcel van den Broek.

Supervision: Niels G. A. Kuijpers, Jack T. Pronk, Jean-Marc G. Daran.

Writing – original draft: Nick Brouwers, Arthur R. Gorter de Vries, Niels G. A. Kuijpers, Jack T. Pronk, Jean-Marc G. Daran.

Writing – review & editing: Nick Brouwers, Arthur R. Gorter de Vries, Niels G. A. Kuijpers, Jack T. Pronk, Jean-Marc G. Daran.

References

1. Libkind D, Hittinger CT, Valério E, Gonçalves C, Dover J, et al. (2011) Microbe domestication and the identification of the wild genetic stock of lager-brewing yeast. *Proc Natl Acad Sci U S A*: 201105430.
2. Sampaio JP (2018) Microbe Profile: *Saccharomyces eubayanus*, the missing link to lager beer yeasts. *Microbiology* 164: 1069–1071. <https://doi.org/10.1099/mic.0.000677> PMID: 30175956
3. Dequin S (2001) The potential of genetic engineering for improving brewing, wine-making and baking yeasts. *Appl Environ Microbiol* 56: 577–588.
4. Peris D, Sylvester K, Libkind D, Gonçalves P, Sampaio JP, et al. (2014) Population structure and reticulate evolution of *Saccharomyces eubayanus* and its lager-brewing hybrids. *Mol Ecol* 23: 2031–2045. <https://doi.org/10.1111/mec.12702> PMID: 24612382
5. Bing J, Han P-J, Liu W-Q, Wang Q-M, Bai F-Y (2014) Evidence for a Far East Asian origin of lager beer yeast. *Curr Biol* 24: R380–R381. <https://doi.org/10.1016/j.cub.2014.04.031> PMID: 24845661
6. Gayevskiy V, Goddard MR (2016) *Saccharomyces eubayanus* and *Saccharomyces arboricola* reside in North Island native New Zealand forests. *Environ Microbiol* 18: 1137–1147. <https://doi.org/10.1111/1462-2920.13107> PMID: 26522264
7. Zastrow C, Hollatz C, De Araujo P, Stambuk B (2001) Maltotriose fermentation by *Saccharomyces cerevisiae*. *J Ind Microbiol Biotechnol* 27: 34–38. <https://doi.org/10.1038/sj/jim/7000158> PMID: 11598808
8. Hebly M, Brickwedde A, Bolat I, Driessen MR, de Hulster EA, et al. (2015) *S. cerevisiae* × *S. eubayanus* interspecific hybrid, the best of both worlds and beyond. *FEMS Yeast Res* 15: pii: fov005. <https://doi.org/10.1093/femsyr/fov005> PMID: 25743788.
9. Brickwedde A, Brouwers N, van den Broek M, Gallego Murillo JS, Fraiture JL, et al. (2018) Structural, physiological and regulatory analysis of maltose transporter genes in *Saccharomyces eubayanus* CBS 12357T. *Front Microbiol* 9: 1786. <https://doi.org/10.3389/fmicb.2018.01786> PMID: 30147677
10. Gallone B, Steensels J, Prah T, Soriaga L, Saels V, et al. (2016) Domestication and Divergence of *Saccharomyces cerevisiae* Beer Yeasts. *Cell* 166: 1397–1410 e1316. <https://doi.org/10.1016/j.cell.2016.08.020> PMID: 27610566
11. Alves SL, Herberts RA, Hollatz C, Trichez D, Miletto LC, et al. (2008) Molecular analysis of maltotriose active transport and fermentation by *Saccharomyces cerevisiae* reveals a determinant role for the

- AGT1 permease. *Appl Environ Microbiol* 74: 1494–1501. <https://doi.org/10.1128/AEM.02570-07> PMID: 18203856
12. Chang Y, Dubin R, Perkins E, Michels C, Needleman R (1989) Identification and characterization of the maltose permease in genetically defined *Saccharomyces* strain. *J Bacteriol* 171: 6148–6154. PMID: 2808304
 13. Naumov GI, Naumova ES, Michels C (1994) Genetic variation of the repeated *MAL* loci in natural populations of *Saccharomyces cerevisiae* and *Saccharomyces paradoxus*. *Genetics* 136: 803–812. PMID: 8005435
 14. Charron MJ, Read E, Haut SR, Michels CA (1989) Molecular evolution of the telomere-associated *MAL* loci of *Saccharomyces*. *Genetics* 122: 307–316. PMID: 2548922
 15. Voordeckers K, Brown CA, Vanneste K, van der Zande E, Voet A, et al. (2012) Reconstruction of ancestral metabolic enzymes reveals molecular mechanisms underlying evolutionary innovation through gene duplication. *PLoS biology* 10: e1001446. <https://doi.org/10.1371/journal.pbio.1001446> PMID: 23239941
 16. Marques WL, Mans R, Marella ER, Cordeiro RL, van den Broek M, et al. (2017) Elimination of sucrose transport and hydrolysis in *Saccharomyces cerevisiae*: a platform strain for engineering sucrose metabolism. *FEMS Yeast Res* 17: fox006 <https://doi.org/10.1093/femsyr/fox006> PMID: 28087672
 17. Han EK, Cotty F, Sottas C, Jiang H, Michels CA (1995) Characterization of *AGT1* encoding a general α -glucoside transporter from *Saccharomyces*. *Mol Microbiol* 17: 1093–1107. PMID: 8594329
 18. Stambuk BU, da Silva MA, Panek AD, de Araujo PS (1999) Active α -glucoside transport in *Saccharomyces cerevisiae*. *FEMS Microbiol Lett* 170: 105–110. <https://doi.org/10.1111/j.1574-6968.1999.tb13361.x> PMID: 9919658
 19. Baker EP, Hittinger CT (2018) Evolution of a novel chimeric maltotriose transporter in *Saccharomyces eubayanus* from parent proteins unable to perform this function. *bioRxiv*: 431171.
 20. Baker E, Wang B, Bellora N, Peris D, Hulfachor AB, et al. (2015) The genome sequence of *Saccharomyces eubayanus* and the domestication of lager-brewing yeasts. *Mol Biol Evol* 32: 2818–2831. <https://doi.org/10.1093/molbev/msv168> PMID: 26269586
 21. Salema-Oom M, Pinto VV, Gonçalves P, Spencer-Martins I (2005) Maltotriose utilization by industrial *Saccharomyces* strains: characterization of a new member of the α -glucoside transporter family. *Appl Environ Microbiol* 71: 5044–5049. <https://doi.org/10.1128/AEM.71.9.5044-5049.2005> PMID: 16151085
 22. Dietvorst J, Londesborough J, Steensma H (2005) Maltotriose utilization in lager yeast strains: *MTT1* encodes a maltotriose transporter. *Yeast* 22: 775–788. <https://doi.org/10.1002/yea.1279> PMID: 16088872
 23. Kupiec M (2014) Biology of telomeres: lessons from budding yeast. *FEMS Microbiol Rev* 38: 144–171. <https://doi.org/10.1111/1574-6976.12054> PMID: 24754043
 24. Louis EJ, Haber JE (1992) The structure and evolution of subtelomeric Y repeats in *Saccharomyces cerevisiae*. *Genetics* 131: 559–574. PMID: 1628806
 25. Louis EJ (1995) The chromosome ends of *Saccharomyces cerevisiae*. *Yeast* 11: 1553–1573. <https://doi.org/10.1002/yea.320111604> PMID: 8720065
 26. Song W, Dominska M, Greenwell PW, Petes TD (2014) Genome-wide high-resolution mapping of chromosome fragile sites in *Saccharomyces cerevisiae*. *Proc Natl Acad Sci U S A*: 201406847.
 27. Pryde FE, Huckle TC, Louis EJ (1995) Sequence analysis of the right end of chromosome XV in *Saccharomyces cerevisiae*: an insight into the structural and functional significance of sub-telomeric repeat sequences. *Yeast* 11: 371–382. <https://doi.org/10.1002/yea.320110410> PMID: 7785338
 28. Brown CA, Murray AW, Verstrepen KJ (2010) Rapid expansion and functional divergence of subtelomeric gene families in yeasts. *Curr Biol* 20: 895–903. <https://doi.org/10.1016/j.cub.2010.04.027> PMID: 20471265
 29. Bergström A, Simpson JT, Salinas F, Barré B, Parts L, et al. (2014) A high-definition view of functional genetic variation from natural yeast genomes. *Mol Biol Evol* 31: 872–888. <https://doi.org/10.1093/molbev/msu037> PMID: 24425782
 30. Dunn B, Richter C, Kvitik DJ, Pugh T, Sherlock G (2012) Analysis of the *Saccharomyces cerevisiae* pan-genome reveals a pool of copy number variants distributed in diverse yeast strains from differing industrial environments. *Genome Res* 22:908–24. <https://doi.org/10.1101/gr.130310.111> PMID: 22369888.
 31. Anderson MZ, Wigen LJ, Burrack LS, Berman J (2015) Real-time evolution of a subtelomeric gene family in *Candida albicans*. *Genetics*: genetics. 115.177451.
 32. Taylor JS, Raes J (2004) Duplication and divergence: the evolution of new genes and old ideas. *Annu Rev Genet* 38: 615–643. <https://doi.org/10.1146/annurev.genet.38.072902.092831> PMID: 15568988

33. Voordeckers K, Verstrepen KJ (2015) Experimental evolution of the model eukaryote *Saccharomyces cerevisiae* yields insight into the molecular mechanisms underlying adaptation. *Curr Opin Biotechnol* 28: 1–9.
34. Ohno S, Wolf U, Atkin NB (1968) Evolution from fish to mammals by gene duplication. *Hereditas* 59: 169–187. PMID: [5662632](#)
35. Ohno S. Gene duplication and the uniqueness of vertebrate genomes circa 1970–1999; 1999. Elsevier. pp. 517–522.
36. Force A, Lynch M, Pickett FB, Amores A, Yan Y-I, et al. (1999) Preservation of duplicate genes by complementary, degenerative mutations. *Genetics* 151: 1531–1545. PMID: [10101175](#)
37. Lynch M, Force A (2000) The probability of duplicate gene preservation by subfunctionalization. *Genetics* 154: 459–473. PMID: [10629003](#)
38. Tang Y-C, Amon A (2013) Gene copy-number alterations: a cost-benefit analysis. *Cell* 152: 394–405. <https://doi.org/10.1016/j.cell.2012.11.043> PMID: [23374337](#)
39. Christiaens JF, Van Mulders SE, Duitama J, Brown CA, Ghequire MG, et al. (2012) Functional divergence of gene duplicates through ectopic recombination. *EMBO Rep* 13: 1145–1151. <https://doi.org/10.1038/embor.2012.157> PMID: [23070367](#)
40. He X, Zhang J (2005) Rapid subfunctionalization accompanied by prolonged and substantial neofunctionalization in duplicate gene evolution. *Genetics* 169: 1157–1164. <https://doi.org/10.1534/genetics.104.037051> PMID: [15654095](#)
41. Rastogi S, Liberles DA (2005) Subfunctionalization of duplicated genes as a transition state to neofunctionalization. *BMC Evol Biol* 5: 28. <https://doi.org/10.1186/1471-2148-5-28> PMID: [15831095](#)
42. Deng C, Cheng C-HC, Ye H, He X, Chen L (2010) Evolution of an antifreeze protein by neofunctionalization under escape from adaptive conflict. *Proc Natl Acad Sci U S A*: 201007883.
43. Des Marais DL, Rausher MD (2008) Escape from adaptive conflict after duplication in an anthocyanin pathway gene. *Nature* 454: 762. <https://doi.org/10.1038/nature07092> PMID: [18594508](#)
44. Hittinger CT, Carroll SB (2007) Gene duplication and the adaptive evolution of a classic genetic switch. *Nature* 449: 677. <https://doi.org/10.1038/nature06151> PMID: [17928853](#)
45. Mans R, Daran J-MG, Pronk JT (2018) Under pressure: Evolutionary engineering of yeast strains for improved performance in fuels and chemicals production. *Curr Opin Biotechnol* 50: 47–56. <https://doi.org/10.1016/j.copbio.2017.10.011> PMID: [29156423](#)
46. Bachmann H, Pronk JT, Kleerebezem M, Teusink B (2015) Evolutionary engineering to enhance starter culture performance in food fermentations. *Curr Opin Biotechnol* 32: 1–7. <https://doi.org/10.1016/j.copbio.2014.09.003> PMID: [25269887](#)
47. Darwin C (2004) *On the origin of species*, 1859. London: Routledge.
48. Yona AH, Manor YS, Herbst RH, Romano GH, Mitchell A, et al. (2012) Chromosomal duplication is a transient evolutionary solution to stress. *Proc Natl Acad Sci U S A* 109: 21010–21015. <https://doi.org/10.1073/pnas.1211150109> PMID: [23197825](#)
49. Gresham D, Desai MM, Tucker CM, Jenq HT, Pai DA, et al. (2008) The repertoire and dynamics of evolutionary adaptations to controlled nutrient-limited environments in yeast. *PLoS Genet* 4: e1000303. <https://doi.org/10.1371/journal.pgen.1000303> PMID: [19079573](#)
50. González-Ramos D, Gorter de Vries AR, Grijsseels SS, Berkum MC, Swinnen S, et al. (2016) A new laboratory evolution approach to select for constitutive acetic acid tolerance in *Saccharomyces cerevisiae* and identification of causal mutations. *Biotechnol Biofuels* 9: 173. <https://doi.org/10.1186/s13068-016-0583-1> PMID: [27525042](#)
51. Caspeta L, Chen Y, Ghiaci P, Feizi A, Buskov S, et al. (2014) Altered sterol composition renders yeast thermotolerant. *Science* 346: 75–78. <https://doi.org/10.1126/science.1258137> PMID: [25278608](#)
52. Papapetridis I, Verhoeven MD, Wiersma SJ, Goudriaan M, van Maris AJA, et al. (2018) Laboratory evolution for forced glucose-xylose co-consumption enables identification of mutations that improve mixed-sugar fermentation by xylose-fermenting *Saccharomyces cerevisiae*. *FEMS Yeast Res* 18: foy056. <https://doi.org/10.1093/femsyr/foy056> PMID: [29771304](#)
53. Verhoeven MD, Bracher JM, Nijland JG, Bouwknegt J, Daran J-MG, et al. (2018) Laboratory evolution of a glucose-phosphorylation-deficient, arabinose-fermenting *S. cerevisiae* strain reveals mutations in *GAL2* that enable glucose-insensitive l-arabinose uptake. *FEMS Yeast Res* 18: foy062 <https://doi.org/10.1093/femsyr/foy062> PMID: [29860442](#).
54. Hong K-K, Vongsangnak W, Vemuri GN, Nielsen J (2011) Unravelling evolutionary strategies of yeast for improving galactose utilization through integrated systems level analysis. *Proc Natl Acad Sci U S A* 108: 12179–12184. <https://doi.org/10.1073/pnas.1103219108> PMID: [21715660](#)

55. Brickwedde A, van den Broek M, Geertman J-MA, Magalhães F, Kuijpers NG, et al. (2017) Evolutionary engineering in chemostat cultures for improved maltotriose fermentation kinetics in *Saccharomyces pastorianus* lager brewing yeast. *Front Microbiol* 8: 1690. <https://doi.org/10.3389/fmicb.2017.01690> PMID: 28943864
56. Verduyn C, Postma E, Scheffers WA, Van Dijken JP (1992) Effect of benzoic acid on metabolic fluxes in yeasts: a continuous-culture study on the regulation of respiration and alcoholic fermentation. *Yeast* 8: 501–517. <https://doi.org/10.1002/yea.320080703> PMID: 1523884
57. Lam V, Daruwalla K, Henderson P, Jones-Mortimer M (1980) Proton-linked D-xylose transport in *Escherichia coli*. *J Bacteriol* 143: 396–402. PMID: 6995439
58. Henderson R, Poolman B (2017) Proton-solute coupling mechanism of the maltose transporter from *Saccharomyces cerevisiae*. *Sci Rep* 7: 14375. <https://doi.org/10.1038/s41598-017-14438-1> PMID: 29084970
59. Yamashita I, Fukui S (1985) Transcriptional control of the sporulation-specific glucoamylase gene in the yeast *Saccharomyces cerevisiae*. *Mol Cell Biol* 5: 3069–3073. PMID: 3939312
60. Knijnenburg TA, Daran J-MG, van den Broek MA, Daran-Lapujade PAS, de Winde JH, et al. (2009) Combinatorial effects of environmental parameters on transcriptional regulation in *Saccharomyces cerevisiae*: a quantitative analysis of a compendium of chemostat-based transcriptome data. *BMC genomics* 10: 53. <https://doi.org/10.1186/1471-2164-10-53> PMID: 19173729
61. Vidgren V, Huuskonen A, Virtanen H, Ruohonen L, Londesborough J (2009) Improved fermentation performance of a lager yeast after repair of its *AGT1* maltose and maltotriose transporter genes. *Appl Environ Microbiol* 75: 2333–2345. <https://doi.org/10.1128/AEM.01558-08> PMID: 19181838
62. Nakao Y, Kanamori T, Itoh T, Kodama Y, Rainieri S, et al. (2009) Genome sequence of the lager brewing yeast, an interspecies hybrid. *DNA Res* 16: 115–129. <https://doi.org/10.1093/dnares/dsp003> PMID: 19261625
63. Vidgren V, Londesborough J (2012) Characterization of the *Saccharomyces bayanus*-type *AGT1* transporter of lager yeast. *J Inst Brew* 118: 148–151.
64. Cousseau F, Alves S Jr, Trichez D, Stambuk B (2013) Characterization of maltotriose transporters from the *Saccharomyces eubayanus* subgenome of the hybrid *Saccharomyces pastorianus* lager brewing yeast strain Weihenstephan 34/70. *Lett Appl Microbiol* 56: 21–29. <https://doi.org/10.1111/lam.12011> PMID: 23061413
65. Nguyen H-V, Legras J-L, Neuvéglise C, Gaillardin C (2011) Deciphering the hybridisation history leading to the lager lineage based on the mosaic genomes of *Saccharomyces bayanus* strains NBRC1948 and CBS380T. *PLoS One* 6: e25821. <https://doi.org/10.1371/journal.pone.0025821> PMID: 21998701
66. Cherry JM, Hong EL, Amundsen C, Balakrishnan R, Binkley G, et al. (2011) *Saccharomyces* Genome Database: the genomics resource of budding yeast. *Nucleic Acids Res* 40: D700–D705. <https://doi.org/10.1093/nar/gkr1029> PMID: 22110037
67. Yan N (2015) Structural biology of the major facilitator superfamily transporters. *Annu Rev Biophys* 44: 257–283. <https://doi.org/10.1146/annurev-biophys-060414-033901> PMID: 26098515
68. Smit A, Moses S, Pretorius I, Cordero Otero R (2008) The Thr⁵⁰⁵ and Ser⁵⁵⁷ residues of the *AGT1*-encoded α -glucoside transporter are critical for maltotriose transport in *Saccharomyces cerevisiae*. *J Appl Microbiol* 104: 1103–1111. <https://doi.org/10.1111/j.1365-2672.2007.03671.x> PMID: 18179544
69. Blount ZD, Barrick JE, Davidson CJ, Lenski RE (2012) Genomic analysis of a key innovation in an experimental *Escherichia coli* population. *Nature* 489: 513. <https://doi.org/10.1038/nature11514> PMID: 22992527
70. Mugnier MR, Cross GA, Papavasiliou FN (2015) The *in vivo* dynamics of antigenic variation in *Trypanosoma brucei*. *Science* 347: 1470–1473. <https://doi.org/10.1126/science.aaa4502> PMID: 25814582
71. Hall JP, Wang H, Barry JD (2013) Mosaic VSGs and the scale of *Trypanosoma brucei* antigenic variation. *PLoS Pathog* 9: e1003502. <https://doi.org/10.1371/journal.ppat.1003502> PMID: 23853603
72. Boothroyd CE, Dreesen O, Leonova T, Ly KI, Figueiredo LM, et al. (2009) A yeast-endonuclease-generated DNA break induces antigenic switching in *Trypanosoma brucei*. *Nature* 459: 278. <https://doi.org/10.1038/nature07982> PMID: 19369939
73. Jackson AP, Berry A, Aslett M, Allison HC, Burton P, et al. (2012) Antigenic diversity is generated by distinct evolutionary mechanisms in African trypanosome species. *Proc Natl Acad Sci U S A* 109: 3416–3421. <https://doi.org/10.1073/pnas.1117313109> PMID: 22331916
74. Hovel-Miner G, Mugnier MR, Goldwater B, Cross GA, Papavasiliou FN (2016) A conserved DNA repeat promotes selection of a diverse repertoire of *Trypanosoma brucei* surface antigens from the genomic archive. *PLoS Genet* 12: e1005994. <https://doi.org/10.1371/journal.pgen.1005994> PMID: 27149665

75. Gibbs MD, Nevalainen KH, Bergquist PL (2001) Degenerate oligonucleotide gene shuffling (DOGS): a method for enhancing the frequency of recombination with family shuffling. *Gene* 271: 13–20. PMID: [11410361](https://pubmed.ncbi.nlm.nih.gov/11410361/)
76. Stemmer WP (1994) Rapid evolution of a protein in vitro by DNA shuffling. *Nature* 370: 389. <https://doi.org/10.1038/370389a0> PMID: [8047147](https://pubmed.ncbi.nlm.nih.gov/8047147/)
77. Cherry JR, Fidantsef AL (2003) Directed evolution of industrial enzymes: an update. *Curr Opin Biotechnol* 14: 438–443. PMID: [12943855](https://pubmed.ncbi.nlm.nih.gov/12943855/)
78. Rogers RL, Bedford T, Lyons AM, Hartl DL (2010) Adaptive impact of the chimeric gene Quetzalcoatl in *Drosophila melanogaster*. *Proc Natl Acad Sci U S A* 107: 10943–10948. <https://doi.org/10.1073/pnas.1006503107> PMID: [20534482](https://pubmed.ncbi.nlm.nih.gov/20534482/)
79. Peter J, De Chiara M, Friedrich A, Yue JX, Pflieger D, et al. (2018) Genome evolution across 1,011 *Saccharomyces cerevisiae* isolates. *Nature* 556: 339–344. <https://doi.org/10.1038/s41586-018-0030-5> PMID: [29643504](https://pubmed.ncbi.nlm.nih.gov/29643504/)
80. Dunn B, Paulish T, Stanbery A, Piotrowski J, Koniges G, et al. (2013) Recurrent rearrangement during adaptive evolution in an interspecific yeast hybrid suggests a model for rapid introgression. *PLoS Genet* 9: e1003366. <https://doi.org/10.1371/journal.pgen.1003366> PMID: [23555283](https://pubmed.ncbi.nlm.nih.gov/23555283/)
81. Hernandez-Rivas R, Hinterberg K, Scherf A (1996) Compartmentalization of genes coding for immunodominant antigens to fragile chromosome ends leads to dispersed subtelomeric gene families and rapid gene evolution in *Plasmodium falciparum*. *Mol Biochem Parasitol* 78: 137–148. PMID: [8813684](https://pubmed.ncbi.nlm.nih.gov/8813684/)
82. Carlson M, Celenza JL, Eng FJ (1985) Evolution of the dispersed *SUC* gene family of *Saccharomyces* by rearrangements of chromosome telomeres. *Mol Cell Biol* 5: 2894–2902. PMID: [3018485](https://pubmed.ncbi.nlm.nih.gov/3018485/)
83. Jordan P, Choe J-Y, Boles E, Oreb M (2016) Hxt13, Hxt15, Hxt16 and Hxt17 from *Saccharomyces cerevisiae* represent a novel type of polyol transporters. *Sci Rep* 6: 23502. <https://doi.org/10.1038/srep23502> PMID: [26996892](https://pubmed.ncbi.nlm.nih.gov/26996892/)
84. Naumov GI, Naumova ES, Louis EJ (1995) Genetic mapping of the α -galactosidase *MEL* gene family on right and left telomeres of *Saccharomyces cerevisiae*. *Yeast* 11: 481–483. <https://doi.org/10.1002/yea.320110512> PMID: [7597853](https://pubmed.ncbi.nlm.nih.gov/7597853/)
85. Teste M-A, François JM, Parrou J-L (2010) Characterization of a new multigene family encoding isomaltases in the yeast *Saccharomyces cerevisiae*: the *IMA* family. *J Biol Chem* 285:26815–24. <https://doi.org/10.1074/jbc.M110> PMID: [20562106](https://pubmed.ncbi.nlm.nih.gov/20562106/)
86. Denayrolles M, de Villechenon EP, Lonvaud-Funel A, Aigle M (1997) Incidence of *SUC-RTM* telomeric repeated genes in brewing and wild wine strains of *Saccharomyces*. *Curr Genet* 31: 457–461. PMID: [9211787](https://pubmed.ncbi.nlm.nih.gov/9211787/)
87. Teunissen A, Steensma H (1995) The dominant flocculation genes of *Saccharomyces cerevisiae* constitute a new subtelomeric gene family. *Yeast* 11: 1001–1013. <https://doi.org/10.1002/yea.320111102> PMID: [7502576](https://pubmed.ncbi.nlm.nih.gov/7502576/)
88. Verstrepen KJ, Klis FM (2006) Flocculation, adhesion and biofilm formation in yeasts. *Mol Microbiol* 60: 5–15. <https://doi.org/10.1111/j.1365-2958.2006.05072.x> PMID: [16556216](https://pubmed.ncbi.nlm.nih.gov/16556216/)
89. Istace B, Friedrich A, d'Agata L, Faye S, Payen E, et al. (2017) *de novo* assembly and population genomic survey of natural yeast isolates with the Oxford Nanopore MinION sequencer. *Gigascience* 6: 1–13.
90. Salazar AN, Gorter de Vries AR, van den Broek M, Wijsman M, de la Torre Cortés P, et al. (2017) Nanopore sequencing enables near-complete *de novo* assembly of *Saccharomyces cerevisiae* reference strain CEN. PK113-7D. *FEMS Yeast Res* 17 fox074. <https://doi.org/10.1093/femsyr/fox074> PMID: [28961779](https://pubmed.ncbi.nlm.nih.gov/28961779/)
91. Guimaraes PM, François J, Parrou JL, Teixeira JA, Domingues L (2008) Adaptive evolution of a lactose-consuming *Saccharomyces cerevisiae* recombinant. *Appl Environ Microbiol* 74: 1748–1756. <https://doi.org/10.1128/AEM.00186-08> PMID: [18245248](https://pubmed.ncbi.nlm.nih.gov/18245248/)
92. Boles E, Oreb M (2018) A Growth-Based Screening System for Hexose Transporters in Yeast. *Methods Mol Biol* 1713: 123. https://doi.org/10.1007/978-1-4939-7507-5_10 PMID: [29218522](https://pubmed.ncbi.nlm.nih.gov/29218522/)
93. Varzakas TH, Arvanitoyannis IS, Baltas H (2007) The politics and science behind GMO acceptance. *Crit Rev Food Sci Nutr* 47: 335–361. <https://doi.org/10.1080/10408390600762696> PMID: [17457721](https://pubmed.ncbi.nlm.nih.gov/17457721/)
94. Zheng X, D'Amore T, Russell I, Stewart G (1994) Factors influencing maltotriose utilization during brewery wort fermentations. *J Am Soc Brew Chem* 52: 41–47.
95. Verstrepen KJ, Derdelinckx G, Dufour J-P, Winderickx J, Thevelein JM, et al. (2003) Flavor-active esters: adding fruitiness to beer. *J Biosci Bioeng* 96: 110–118. PMID: [16233495](https://pubmed.ncbi.nlm.nih.gov/16233495/)
96. García AI, García LA, Díaz M (1994) Modelling of diacetyl production during beer fermentation. *J Inst Brew* 100: 179–183.

97. Diderich JA, Weening SM, van den Broek M, Pronk JT, Daran J-MG (2018) Selection of Pof-*Saccharomyces eubayanus* Variants for the Construction of *S. cerevisiae* × *S. eubayanus* Hybrids With Reduced 4-Vinyl Guaiacol Formation. *Front Microbiol* 9:1640. <https://doi.org/10.3389/fmicb.2018.01640> PMID: 30100898.
98. Mertens S, Steensels J, Saels V, De Rouck G, Aerts G, et al. (2015) A large set of newly created inter-specific yeast hybrids increases aromatic diversity in lager beers. *Appl Environ Microbiol* 81:8202–14. <https://doi.org/10.1128/AEM.02464> PMID: 26407881.
99. Hittinger CT, Steele JL, Ryder DS (2018) Diverse yeasts for diverse fermented beverages and foods. *Curr Opin Biotechnol* 49: 199–206. <https://doi.org/10.1016/j.copbio.2017.10.004> PMID: 29102814
100. Krogerus K, Magalhães F, Vidgren V, Gibson B (2017) Novel brewing yeast hybrids: creation and application. *Appl Microbiol Biotechnol* 101: 65–78. <https://doi.org/10.1007/s00253-016-8007-5> PMID: 27885413
101. Bellon JR, Eglinton JM, Siebert TE, Pollnitz AP, Rose L, et al. (2011) Newly generated interspecific wine yeast hybrids introduce flavour and aroma diversity to wines. *Appl Microbiol Biotechnol* 91: 603–612. <https://doi.org/10.1007/s00253-011-3294-3> PMID: 21538112
102. Peris D, Moriarty RV, Alexander WG, Baker E, Sylvester K, et al. (2017) Hybridization and adaptive evolution of diverse *Saccharomyces* species for cellulosic biofuel production. *Biotechnol Biofuels* 10: 78. <https://doi.org/10.1186/s13068-017-0763-7> PMID: 28360936
103. Van den Broek M, Bolat I, Nijkamp JF, Ramos E, Luttk MAH, et al. (2015) Chromosomal copy number variation in *Saccharomyces pastorianus* evidence for extensive genome dynamics in industrial lager brewing strains. *Appl Environ Microbiol* 81:6253–67. <https://doi.org/10.1128/AEM.01263-15> PMID: 26150454.
104. Solis-Escalante D, Kuijpers NG, Nadine B, Bolat I, Bosman L, et al. (2013) amdSYM, a new dominant recyclable marker cassette for *Saccharomyces cerevisiae*. *FEMS Yeast Res* 13: 126–139. <https://doi.org/10.1111/1567-1364.12024> PMID: 23253382
105. Li H, Durbin R (2010) Fast and accurate long-read alignment with Burrows–Wheeler transform. *Bioinformatics* 26: 589–595. <https://doi.org/10.1093/bioinformatics/btp698> PMID: 20080505
106. Li H, Handsaker B, Wysoker A, Fennell T, Ruan J, et al. (2009) The sequence alignment/map format and SAMtools. *Bioinformatics* 25: 2078–2079. <https://doi.org/10.1093/bioinformatics/btp352> PMID: 19505943
107. Walker BJ, Abeel T, Shea T, Priest M, Abouelliel A, et al. (2014) Pilon: an integrated tool for comprehensive microbial variant detection and genome assembly improvement. *PLoS One* 9: e112963. <https://doi.org/10.1371/journal.pone.0112963> PMID: 25409509
108. Chen K, Wallis JW, McLellan MD, Larson DE, Kalicki JM, et al. (2009) BreakDancer: an algorithm for high-resolution mapping of genomic structural variation. *Nat Methods* 6: 677. <https://doi.org/10.1038/nmeth.1363> PMID: 19668202
109. Nijkamp JF, van den Broek MA, Geertman J-MA, Reinders MJ, Daran J-MG, et al. (2012) De novo detection of copy number variation by co-assembly. *Bioinformatics* 28: 3195–3202. <https://doi.org/10.1093/bioinformatics/bts601> PMID: 23047563
110. Simpson JT, Wong K, Jackman SD, Schein JE, Jones SJ, et al. (2009) ABySS: a parallel assembler for short read sequence data. *Genome Res* 19:1117–23. <https://doi.org/10.1101/gr.089532.108> PMID: 19251739
111. Robinson JT, Thorvaldsdóttir H, Winckler W, Guttman M, Lander ES, et al. (2011) Integrative genomics viewer. *Nat Biotechnol* 29: 24. <https://doi.org/10.1038/nbt.1754> PMID: 21221095
112. Koren S, Walenz BP, Berlin K, Miller JR, Bergman NH, et al. (2017) Canu: scalable and accurate long-read assembly via adaptive k-mer weighting and repeat separation. *Genome Res* 27:722–736. <https://doi.org/10.1101/gr.215087> PMID: 28298431.
113. Li H (2018) Minimap2: pairwise alignment for nucleotide sequences. *Bioinformatics* 1: 7.
114. Pengelly RJ, Wheals AE (2013) Rapid identification of *Saccharomyces eubayanus* and its hybrids. *FEMS Yeast Res* 13: 156–161. <https://doi.org/10.1111/1567-1364.12018> PMID: 23110474
115. Muir A, Harrison E, Wheals A (2011) A multiplex set of species-specific primers for rapid identification of members of the genus *Saccharomyces*. *FEMS Yeast Res* 11: 552–563. <https://doi.org/10.1111/j.1567-1364.2011.00745.x> PMID: 22093682
116. Schoch CL, Seifert KA, Huhndorf S, Robert V, Spouge JL, et al. (2012) Nuclear ribosomal internal transcribed spacer (ITS) region as a universal DNA barcode marker for Fungi. *Proc Natl Acad Sci U S A* 109: 6241–6246. <https://doi.org/10.1073/pnas.1117018109> PMID: 22454494
117. Gibson DG, Young L, Chuang R-Y, Venter JC, Hutchison CA III, et al. (2009) Enzymatic assembly of DNA molecules up to several hundred kilobases. *Nat Methods* 6: 343. <https://doi.org/10.1038/nmeth.1318> PMID: 19363495

118. de Kok S, Yilmaz D, Suir E, Pronk JT, Daran J-MG, et al. (2011) Increasing free-energy (ATP) conservation in maltose-grown *Saccharomyces cerevisiae* by expression of a heterologous maltose phosphorylase. *Metab Eng* 13: 518–526. <https://doi.org/10.1016/j.ymben.2011.06.001> PMID: 21684346
119. Bao Z, Xiao H, Liang J, Zhang L, Xiong X, et al. (2014) Homology-integrated CRISPR–Cas (HI-CRISPR) system for one-step multigene disruption in *Saccharomyces cerevisiae*. *ACS Synth Biol* 4: 585–594. <https://doi.org/10.1021/sb500255k> PMID: 25207793
120. Gorter de Vries AR, Groot PA, Broek M, Daran J-MG (2017) CRISPR-Cas9 mediated gene deletions in lager yeast *Saccharomyces pastorianus*. *Microb Cell Fact* 16: 222. <https://doi.org/10.1186/s12934-017-0835-1> PMID: 29207996
121. Biasini M, Bienert S, Waterhouse A, Arnold K, Studer G, et al. (2014) SWISS-MODEL: modelling protein tertiary and quaternary structure using evolutionary information. *Nucleic Acids Res* 42: W252–W258. <https://doi.org/10.1093/nar/gku340> PMID: 24782522
122. Gueux N, Peitsch MC, Schwede T (2009) Automated comparative protein structure modeling with SWISS-MODEL and Swiss-PdbViewer: A historical perspective. *Electrophoresis* 30: S162–S173. <https://doi.org/10.1002/elps.200900140> PMID: 19517507
123. Brouwers N, Gorter de Vries AR, van den Broek M, Weening SM, Elink Schuurman TD, et al. (2018) In vivo recombination of *Saccharomyces eubayanus* maltose-transporter genes yields a chimeric transporter that enables maltotriose fermentation. *bioRxiv* 428839; <https://doi.org/10.1101/428839>